ELECTROSPUN NANOFIBROUS SCAFFOLDS FOR TISSUE ENGINEERING

A THESIS SUBMITTED TO
THE GRADUATE SCHOOL OF NATURAL AND APPLIED SCIENCES
OF
MIDDLE EAST TECHNICAL UNIVERSITY

BY

ALBANA NDREU

IN PARTIAL FULFILLMENT OF THE REQUIREMENTS
FOR
THE DEGREE OF MASTER OF SCIENCE
IN
BIOTECHNOLOGY

JANUARY 2007

Approval of the Graduate School of Natural and Applied Sciences

Prof. Dr. Canan Özgen
Director

I certify that this thesis satisfies all the requirements as a thesis for the degree of Master of Science.

Prof. Dr. Fatih Yıldız
Head of Department

This is to certify that we have read this thesis and that in our opinion it is fully adequate, in scope and quality, as a thesis and for the degree of Master of Science.

Prof. Dr. Nesrin Hasırcı
Co-Supervisor

Prof. Dr. Vasıf Hasırcı
Supervisor

Examining Committee Members

Prof. Dr. Mesude İşcan (METU, BIO) _____

Prof. Dr. Vasıf Hasırcı (METU, BIO) _____

Prof. Dr. Hüseyin A. Öktem (METU, BIO) _____

Prof. Dr. İskender Yılgör (Koç Unv., CHEM) _____

Prof. Dr. Tülin Güray (METU, BIO) _____

I hereby declare that all information in this document has been obtained and presented in accordance with academic rules and ethical conduct. I also declare that, as required by these rules and conduct, I have fully cited and referenced all material and results that are not original to this work.

Name, Last name : Albana NDREU

Signature :

ABSTRACT

ELECTROPSUN NANOFIBROUS SCAFFOLDS FOR TISSUE ENGINEERING

Ndreu, Albana
M.S., Department of Biotechnology
Supervisor : Prof. Dr. Vasıf Hasırcı
Co-Supervisor : Prof. Dr. Nesrin Hasırcı

December 2006, 83 pages

In this study a microbial polyester, poly(3-hydroxybutyrate-co-3-hydroxyvalerate) (PHBV), and its blends were wet or electrospun into fibrous scaffolds for tissue engineering.

Wet spun fiber diameters were in the low micrometer range (10-50 μm). The polymer concentration and the stirring rate affected the properties the most. The optimum concentration was determined as 15% (w/v).

Electrospun fiber diameters, however, were thinner. Solution viscosity, potential, distance between the syringe tip and the collector, and polymer type affected the morphology and the thickness of beads formed on the fibers. Concentration was highly influential; as it increased from 5% to 15% (w/v) fiber diameter increased from 284 ± 133 nm to 2200 ± 716 nm. Increase in potential (from 20 to 50 kV) did not lead to the expected decrease in fiber diameter. The blends of PHBV8 with lactide-based

polymers (PLLA, P(L,DL-LA) and PLGA (50:50)) led to fibers with less beads and more uniform thickness.

I*n vitro studies* using human osteosarcoma cells (SaOs-2) revealed that wet spun fibers were unsuitable because the cells did not spread on them while all the electrospun scaffolds promoted cell growth and penetration. The surface porosities for PHBV10, PHBV15, PHBV-PLLA, PHBV-PLGA (50:50) and PHBV-P(L,DL)LA were 38.0±3.8, 40.1±8.5, 53.8±4.2, 50.0±4.2 and 30.8±2.7%, respectively. Surface modification with oxygen plasma treatment slightly improved the cell proliferation rates.

Consequently, all scaffolds prepared by electrospinning revealed a significant potential for use in bone tissue engineering applications; PHBV-PLLA blend appeared to yield the best results.

Keywords: Tissue Engineering; Extracellular matrix (ECM); Biodegradable; Nanofibers; Wet spinning; Electrospinning.

ÖZ

DOKU MÜHENDİSLİĞİ AMAÇLI ELECTROSPİN EDİLMİŞ NANOFİBRİL TAŞIYICILAR

Ndreu, Albana
Yüksek Lisans, Biyoteknoloji ABD
Tez Yöneticisi : Prof. Dr. Vasıf Hasırcı
Ortak Tez Yöneticisi : Prof. Dr. Nesrin Hasırcı

Aralık 2006, 83 sayfa

Bu çalışmada, mikroorganizmalar tarafından üretilen bir polyester olan poli(3-hidroksibutirat-ko-3-hidroksivalerat) (PHBV) ve bunun karışımları, doku mühendisliğinde kullanılmak üzere "wet spinning" ve "electrospinning" yöntemleriyle lifsi yapılı hücre taşıyıcısı oluşturulmasında kullanılmıştır.

"Wet spinning" yöntemiyle oluşturulan lifsi yapıların çapları 10-50 mikrometre arasında değişmektedir. Boyutu etkileyen en önemli etkenler arasında polimer konsantrasyonu ve karıştırma hızı gelmektedir. En uygun konsantrasyon %15 (w/v) olarak belirlenmiştir.

"Electrospinning" yöntemiyle elde edilen polimerik ipliklerin "wet spinning" yöntemiyle elde edilenlere göre daha ince olduğu gözlenmiştir. Liflerde oluşabilen polimer boğumlarının biçimi ve kalınlığı çözeltinin akışkanlığı, kullanılan potansiyel, uzaklık ve polimer tipi gibi ögelerden etkilenmektedir. Liflerin çapları özellikle polimer konsantrasyonundan büyük ölçüde etkilenmektedir. Konsantrasyonun %5 (w/v)'den %15 (w/v)'e yükseltilmesi

liflerin çapını 284 ± 133 nm'den 2200 ± 716 nm'ye yükseltmiştir. Uygulanan potansiyeldeki artış (20 kV'dan 50 kV'a) lif çapında beklenen azalmayı göstermemiştir. PHBV8 ile laktid kökenli polimerlerin (PLLA, P(L,DL-LA) ve PLGA (50:50)) karışımlarının kullanımı daha az boğumlu ve genel olarak tek düze kalınlıklı liflerin oluşmasını sağlamıştır.

İnsan osteosarkoma hücreleri (SaOs-2) kullanılarak gerçekleştirilen i*n vitro* çalışmalar "wet spinning" tekniğiyle oluşturulan liflerin hücrelerin yayılması açısından uygun olmadığını, "electrospinning" yöntemiyle yapılan taşıyıcıların ise hücrelerin büyümesi ve taşıyıcı içinde yayılması bakımından uygun olduğunu göstermiştir. PHBV10, PHBV15, PHBV-PLLA, PHBV-PLGA (50:50) ve PHBV-P(L,DL)LA ile elde edilen yapıların yüzey gözenekliliği sırasıyla % 38.0 ± 3.8, % 40.1 ± 8.5, % 53.8 ± 4.2, % 50.0 ± 4.2 ve % 30.8 ± 2.7 olarak saptanmıştır. Oksijen plazma tekniğiyle yapılan yüzey değişikliklerinin hücre çoğalma hızını çok az arttırmıştır.

Sonuç olarak, electrospinning" yöntemiyle elde edilen bütün hücre taşıyıcılarının kemik doku mühendisliğinde kullanılma potansiyeline sahip olduğu gösterilmiş ve PHBV-PLLA polimer karışımları kullanılarak hazırlanan taşıyıcıların en iyi sonucu verdiği belirlenmiştir.

Anahtar kelimeler: Doku Mühendisliği; Hücre Dışı Matriks (ECM); Biyobozunur; Nanolifler; Wet spinning; Electrospinning.

To My Family

ACKNOWLEDGEMENTS

I wish to express my sincere gratitude to my supervisor Prof. Dr. Vasıf Hasırcı, for his continuous guidance, support, and help throughout this study.

I would also like to thank Prof. Dr. Nesrin Hasırcı for her contributions to this study as my co-supervisor.

I am very grateful to Prof. Nureddin Ashammakhi and his students Lila Nikkola and Hanna Ylikauppila for their hospitality and kindness during my insightful visit to Institute of Biomaterials (Tampere University of Technology, Finland). It was a very good and fruitful experience for me and I would like to thank their staff for supporting all the necessary equipments required to handle my experiments.

I am grateful to my husband Dr. Ismail Halili for his help, support and kindness during all my MSc. studies.

I would like to thank my labmates for their help, support and understanding especially in my hard days; Pınar Yılgör, Nihan Öztürk, Engin Vrana, Halime Kenar, Deniz Yücel, Buket Başmanav, Pınar Zorlutuna, Erkin Aydın and Dr. Mathilde Hindie; they have all contributed to this study in some way.

I am grateful to the EU FP6 "Expertissues" Project, through which the research was funded.

I would finally like to acknowledge METU Central Laboratory for analyses done in their facilities.

TABLE OF CONTENTS

LIST OF TABLES

Tables

LIST OF FIGURES

Figures

NOMENCLATURE

Abbreviations

CLSM	Confocal Laser Scanning Microscope
DMEM	Dulbecco's Modified Eagle's Medium
DAPI	4',6-Diamidino-2-phenylindole
ECM	Extracellular Matrix
FITC	Fluorescein Isothiocyanate
MTS	3-(4,5-dimethylthiazol-2-yl)-5-(3-carboxymethoxyphenyl)-2-(4-sulfophenyl)-2H-tetrazolium
OD	Optical Density
PBS	Phosphate Buffered Saline
PHBV	Poly(3-hydroxybutyrate-co-hydroxyvalerate)
PLLA	Poly(L-lactic acid)
P(L,DL)LA	Poly(L,DL-lactic acid)
PLGA (50:50)	Poly(lactic acid-co-glycolic acid) (50:50)
PLGA (75:25)	Poly(lactic acid-co-glycolic acid) (75:25)
PMS	Phenazine Methosulfate
SEM	Scanning Electron Microscope

CHAPTER 1

INTRODUCTION

1.1. Nanotechnology

Nanotechnology is an emerging interdisciplinary technology that influenced many areas during the last decade, including mechanics, materials science, electronics, medicine, optics, energy, aerospace and biomedical engineering. The original version of 'Nano' is 'nanos', meaning 'dwarf'. The diameter of human hair is about 10^5 nanometers.

The first known use of nanotechnology is 'atomic assembly' and the first article was published by the physicist Richard Feynman [1]. The essence of this new technology is the creation and utilization of surfaces, materials and devices at the molecular level [2].

The properties of substances change dramatically when their size is reduced to the nanometric level. For instance, ceramics, which normally are brittle, can easily be made deformable when their grain size is reduced to the low nanometer range [2]. A small amount of nanosize materials can be mixed with a polymer matrix and improve the performance of resultant system to an unprecedented level. There has also been a significant increase in nanotechnology-based biomedical applications, especially in tissue engineering. Advances such as these have led to the large research funds, activity, and attention devoted to nanotechnology.

1.2. Tissue Engineering

Tissue engineering is an outgrowth of the biomaterials field, which involves producing tissue substitutes from a variety of biodegradable polymers and

cells to create the target tissue whose structural characteristics and function need to be restored. It is an interdisciplinary field that combines the knowledge of many sciences ranging from biology to materials science and medicine [3]. It is a subject of intensive research for human health care systems.

Human body is a complex and well organized system consisting of tissues and organs. Nutrients, oxygen and the suitable environment for the cell growth is available in the tissues. The extracellular matrix (ECM), component of tissues, is a complex structure surrounding and supporting the cells within the mammalian tissues. It is composed of 3 major classes of biomolecules: (1) *structural proteins,* mainly collagen and elastin, (2) *specialized proteins* such as fibrillin, fibronectin and laminin, and (3) *proteoglycans* which are proteins to which long chains of repeating disaccharide units called glycosaminoglycans (GAGs), are attached.

Cell-extracellular matrix (ECM) and cell-cell interactions determine the ability of cells to build tissues and maintain tissue-specific functions. An important objective of tissue engineering is the recreation of an appropriate cellular environment that helps in control and regulation of cell functions [4]. During the last decade intensive research was conducted in this field.

There are two main components of a tissue engineered product; cells and the carrier. The success rate of tissue engineering depends in part on carriers which are designed as scaffolds. The best approach for achieving this is to design the scaffold, preferably a biodegradable one, to mimic the functions and structure of the naturally existing ECM. In constructing an engineered tissue, initially the cells are isolated from the donor tissue and cultured under *in vitro* conditions *(Fig. 1*). A polymeric scaffold is designed by means of various processing methods such as solvent casting, salt leaching, phase separation, self-assembly, gas foaming and electrospinning. The cells are then seeded and cultured on this scaffold (or cell carrier). In order to imitate the natural environment of cells, the above steps are performed in either static culture conditions or dynamic bioreactor systems [5]. The cells are expected to show a similar behavior to that in the body.

The cells proliferate, migrate, differentiate and remodel the scaffold and the surrounding tissue to achieve healing.

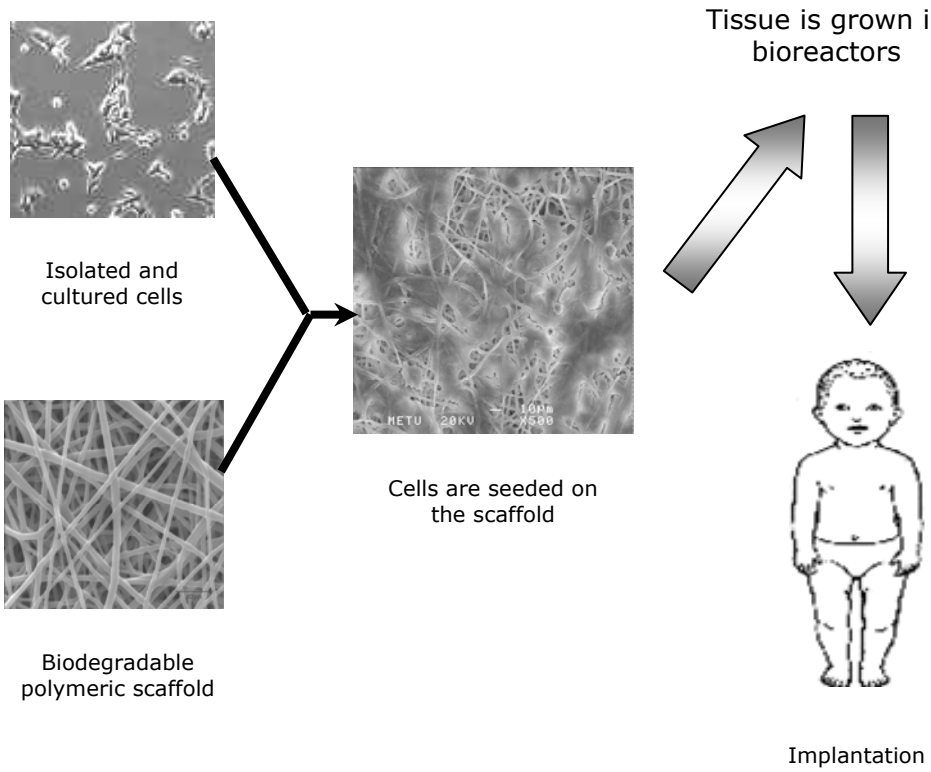

Figure 1. Schematic presentation of tissue engineering methodology.

1.2.1. Scaffold Materials

Since most of the cells are dependent on the scaffold characteristics, biomaterial choice for scaffold design is of great importance for proper adhesion, spreading etc. Polymers are the most suitable scaffold materials due to their flexibility and controllable functional properties. Depending on the requirements of the target tissue, the material is chosen to be either a naturally derived polymer (collagen [6, 7], cellulose [8], chitin [9], starch [10, 11], hyaluronic acid [12], silk fibroin [13] or a synthetic one (poly(lactic acid) [14], poly(glycolic acid) [14, 15], poly(lactide-co-caprolactone) [10, 11, 16], poly(ethylene glycol) [17] and their combinations (Table 1). The former group consists of biodegradable materials whereas the latter can be

either biodegradable or not. Biodegradable materials are preferred as tissue engineering scaffolds since they degrade while the new tissue forms. Another requirement is that the carrier material and the degradation products should be biocompatible so that no adverse body reactions occur when the material degrades in time.

Copolymers have also been utilized in designing tissue engineering scaffolds since polymers with varying crystallinity degrees, and thus, with a range of properties are available. These copolymers still crystallize but have the ability to melt at lower temperatures, making processing easier. PHBV which is a copolymer of 3-hydroxybutyrate (92%) and 3-hydroxyvalerate (8%), was used in the current study. It is advantageous in that it degrades *in vivo* to D-3-hydroxybutyrate, which is a normal constituent of human blood, and to 3-hydroxyvalerate. Its *in vitro* biodegradability [18] and biocompatibility in the presence of various cell lines [19, 20] are reported in the literature.

Choi *et al.* (2004) has demonstrated that even the form of the scaffold affects the results [18]. Higher biodegradability was observed with non-woven, fibrous PHBV8 structures in comparison to films of the same material. Furthermore, the suitability of this nonwoven, fibrous material as a scaffold for tissue engineering [19-22] and its *in vivo* biocompatibility [23] has been demonstrated previously.

Table 1. List of biodegradable and bioerodible polymers that were used in electrospinning to produce nanofibers.

A. Synthetic polymers
Poly(DL-lactide) [24, 25]
Poly(L-lactide) [14, 24, 26, 27, 28, 25, 29]
Poly(ε-caprolactone) [4, 26, 30, 29, 31, 32]
Poly(lactide-*co*-glycolide) 10:90 [14], 65:35 [33], 75:25 [14, 34] or 85:15 [35]
Poly(L-lactide-*co*-ε-caprolactone) 75:25 [36, 37, 38] 70:30, 50:50 or 30:70 [26]
Poly(DL-lactide-*co*-ε-caprolactone) 5:95 [39]
Poly(DL-lactide)-poly(ethylene glycol)-poly(DL-lactide) triblock copolymer [40]
Poly(ethylene glycol)-poly(L-lactide) diblock copolymer [24]
Poly(ethylene glycol)-poly(DL-lactide) diblock copolymer [14, 24]
Poly(ethylene oxide) [17]

Table 1. (continued)

Poly[bis(methylphenoxy)phosphazene] [29]
Poly(vinyl alcohol) coated Poly(p-xylylene) [41]
Poly(ethylene-*co*-vinyl alcohol) [42]
Poly(ε-caprolactone-*co*-ethyl ethylene phosphate) [43, 44]
Poly(ε-caprolactone-*co*-ethyl ethylene phosphate), surface grafted with poly(acrylic acid) [43]
Poly(ε-caprolactone) core coated with collagen shell (from calf skin) [45]
Poly(ester urethane)urea [46]
B. Natural-origined polymers
Silk fibroin [13, 47]
Hyaluronic acid [12]
Cellulose [8]
Oxidised cellulose [17]
Hydroxypropylmethylcellulose [48]
Collagen type I (from calfskin [4, 49, 50] or from human placenta [49]
Collagen type II (from chicken sternae) [51]
Collagen type III (from human placenta) [49]
Gelatin (denatured collagen from bovine skin) [4]
Solubilized alpha-elastin [4]
Tropoelastin (Recombinant human) [4]
Chitin [9]
Chitosan [52]
Poly(3-hydroxybutyrate-co-3-hydroxyvalerate) 8 (%) *
Fibrin [31, 53]
Fibrinogen [53]
C. Blends/Combinations
PLGA 10/90 and PLLA (75:25 w%) [14]
PLGA 25/75 and PEG–PDLLA (85:15 w%) [14]
PDLLA, PLGA 50/50, PDLA-b-PEG-b-PDLA and Lactide (40: 25: 20:15 w%) [15]
PLGA, PEG-b-PDLA diblock copolymer and PLA (80:15:5 w%) [34]
PCL/PVA combination [53]
Silk fibroin and poly(ethylene oxide) [54]
Cellulose and heparin [8]
Starch and PCL (30:70 w/w%) [10, 11]
Poly(3-hydroxybutyrate-co-hydroxyvalerate) and P(L/DL)LA 70:30 (1:1) *
Poly(3-hydroxybutyrate-co-hydroxyvalerate) and PLLA (1:1) *
Poly(3-hydroxybutyrate-co-hydroxyvalerate) and PLGA 75:25 (1:1) *
Poly(3-hydroxybutyrate-co-hydroxyvalerate) and PLGA 50:50 (1:1) *
Collagen type I and III (both from human placenta) 50:50 [49]
Collagen type I (from calf skin), elastin (from ligamentum nuchae), and poly(D,L-lactide-co-glycolide) (45:40:15) [6]
Collagen (type I from calf skin), elastin (from bovine neck ligament) and poly(ethylene oxide) [7]
Collagen-chondroitin sulfate (96:4 and 90:10) [55]
Collagen (type I from calf skin) and poly(ethylene oxide) [7]
Collagen (type I from calf skin) and poly(L-lactide-co-ε-caprolactone) 70:30 (1:1 w/w) [56]
Collagen (type I from calf skin) and poly(ε-caprolactone) [57]

Table 1. (continued)

Collagen (type I from calf skin) and poly(ε-caprolactone) [45]
Gelatin (type B, bovine skin) [58]
Gelatin (type A, porcine skin) and poly(ε-caprolactone) [59]
Elastin (from calf bovine neck ligament) and poly(ethylene oxide) [7]

* : Polymers used in this study

1.2.2. Scaffold Characteristics and Types

As mentioned above, the first step of tissue engineering is the design of a 3-D scaffold that mimics the ECM. Therefore, when designing the scaffolds there are some very important points that should be taken into consideration. One of the most crucial things is that both the carrier material and its degradation products should have proven biodegradability and biocompatibility. Moreover, the scaffold should possess appropriate porosity and permeability to allow the transfer of nutrients necessary for the cells and wastes produced by the cells. A surface chemistry that enables attachment and spreading of cells is also required. The material should have an appropriate degradation rate and mechanical properties so that the artificial material is eliminated in time and different stresses that may develop during new tissue formation can be handled [3, 60]. Finally, the technique that is used to fabricate the scaffolds should not affect the biocompatibility of the material used [61].

To date, scaffolds have been produced in different forms such as films [62, 63], foams [22, 64-66] and fibers [24, 39, 65, 67-69] with widely differing chemistries (*Fig.2*) and a variety of studies ranging from in situ to clinical have been carried out.

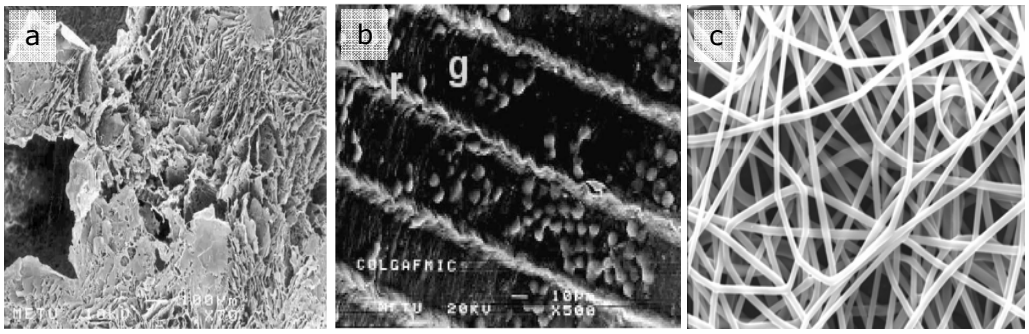

Figure 2. SEM micrographs of various tissue engineering scaffolds. (a) untreated PHBV (6%, w/v) foams with sucrose leaching. Sucrose size range: 75-300 μm [19]; (b) glutaraldehyde crosslinked collagen films showing cell alignment and orientation [70] and (c) PHBV8-P(L/DL)LA (70:30) blend obtained by electrospinning.

All these scaffold types have been tested for their suitability in tissue engineering. Initially, foam and film types were more popular, however, recently there has been an increase in the use of fibrous scaffolds. Some recent studies have shown that cells attach, grow and organize well on nanofibrous structures even though the fiber diameter is smaller than that of the cells [26, 71]. High porosity that allows rapid transfer of nutrients and wastes and the large surface areas that provide sites for the cells to attach are the requirements of a successful scaffold. Furthermore, micro and nano-featured scaffolds with controlled pore size, geometry, dimension and spatial orientation are being intensely investigated. Since fibrous scaffolds with diameters of fibers as small as nanometer scale have been found to be satisfactory for tissue engineering, an extensive research towards developing processes for the fabrication of these fibrous structures is being pursued.

1.3. Micro and Nanofiber Fabrication Methods

Several techniques have been employed in the production of fibrous scaffolds. These are self-assembly, drawing, template synthesis, phase separation, wet spinning, electrospinning and combinations of these [16, 72]. Each of these methods leads to fibers with different properties and

characteristics (*Table 2*). Each of these methods has its own advantages and disadvantages.

Table 2. Relationship between the fiber diameter and process type [16, 72].

Fiber (10-100 μm)	Microfiber (8-100 nm)	Nanofiber (0.5-1 μm)
Dry spinning	Modified melt blown	Self-assembly
Wet spinning	Islands-in-the-sea	Electrospinning
Dry-jet wet spinning	Radial sheath separation	Modified electrospinning
Melt spinning	Multiplayer separate process	
Melt blown		

1.3.1. Self assembly

Known as a 'bottom-up' method it yields fibers with small diameters (less than 100 nm thick and up to few micrometer lengths) and it offers novel properties and functionalities, which cannot be achieved by conventional organic synthesis.

In this process, atoms and molecules arrange themselves through weak, non-covalent interactions (H-bonding, hydrophobic forces, electrostatic interactions) forces into well defined and stable structures [16]. Self assembly of nanofibers refers to the build up of nano-scale fibers from smaller molecules.

Figure 3 shows how small molecules are arranged in a concentric manner, bonds form among the concentrically arranged molecules, and then a nanofiber is formed upon extension of these molecules normal to the plane [73].

The main disadvantage of the method is that it is a complex, long, and extremely elaborate technique with low productivity [74].

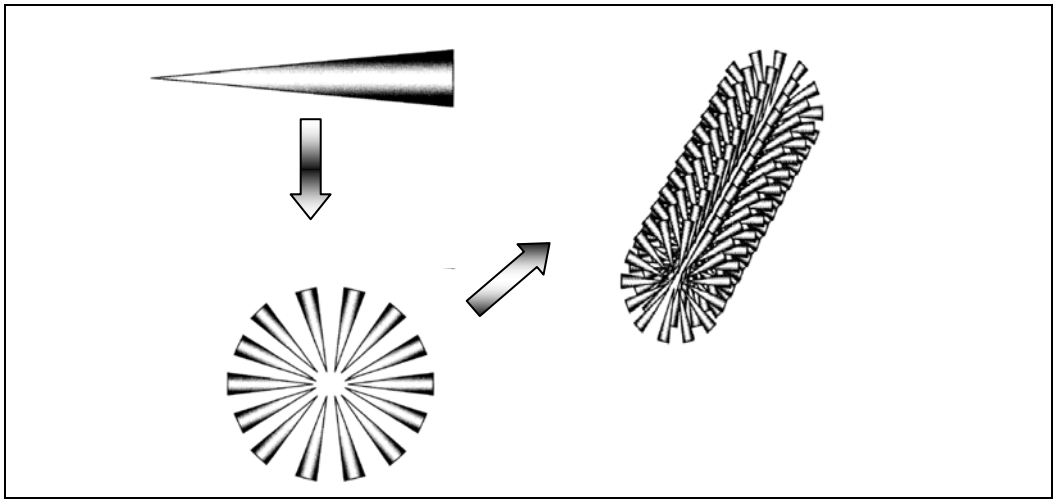

Figure 3. Schematic presentation of self-assembled nanofiber production [74].

1.3.2. Drawing

Dry spinning is a method used to form polymeric fibers from solution. However, instead of precipitating the polymer by dilution or chemical reaction as in wet spinning, solidification is achieved by evaporating the solvent in a stream of air or inert gas. The filaments do not come in contact with a precipitating liquid, eliminating the need for drying and easing solvent recovery. In more details, the polymer is dissolved in a volatile solvent and the solution is pumped through a spinneret composed of numerous holes. As the fibers exit the spinneret, air is used to evaporate the solvent so that the fibers solidify and can be collected on a take up wheel. Stretching of the fibers provides for orientation of the polymer chains along the fiber axis. Dry spun fibers typically have lower void content than wet spun fibers. However, due to their higher density, they have decreased dye-absorption capability. This technique is used only for polymers that cannot be melt spun [75].

Drawing is another method utilized to produce fibers. It is similar to dry spinning and one-by-one single nanofibers can be produced. It requires a minimum amount of equipments, and is a discontinuous process. As shown

in the Figure 4, a micropipette is dipped into a droplet near the solution-solid surface contact line via a micromanipulator. Then the micropipette is withdrawn from the liquid at a certain speed, yielding a nanofiber. These steps are repeated many times on each droplet. The solution viscosity, however, increases with solvent evaporation and some fiber breaking occurs due to instabilities that occur during the process [76].

Drawing process is disadvantageous since it requires solutions of only viscoelastic materials, which can undergo strong deformations that are cohesive enough to withstand the stresses developed during pulling. Moreover, since the fiber size is dependent on the orifice size of the extrusion mould, it is difficult to obtain fibers diameters less than 100 nm.

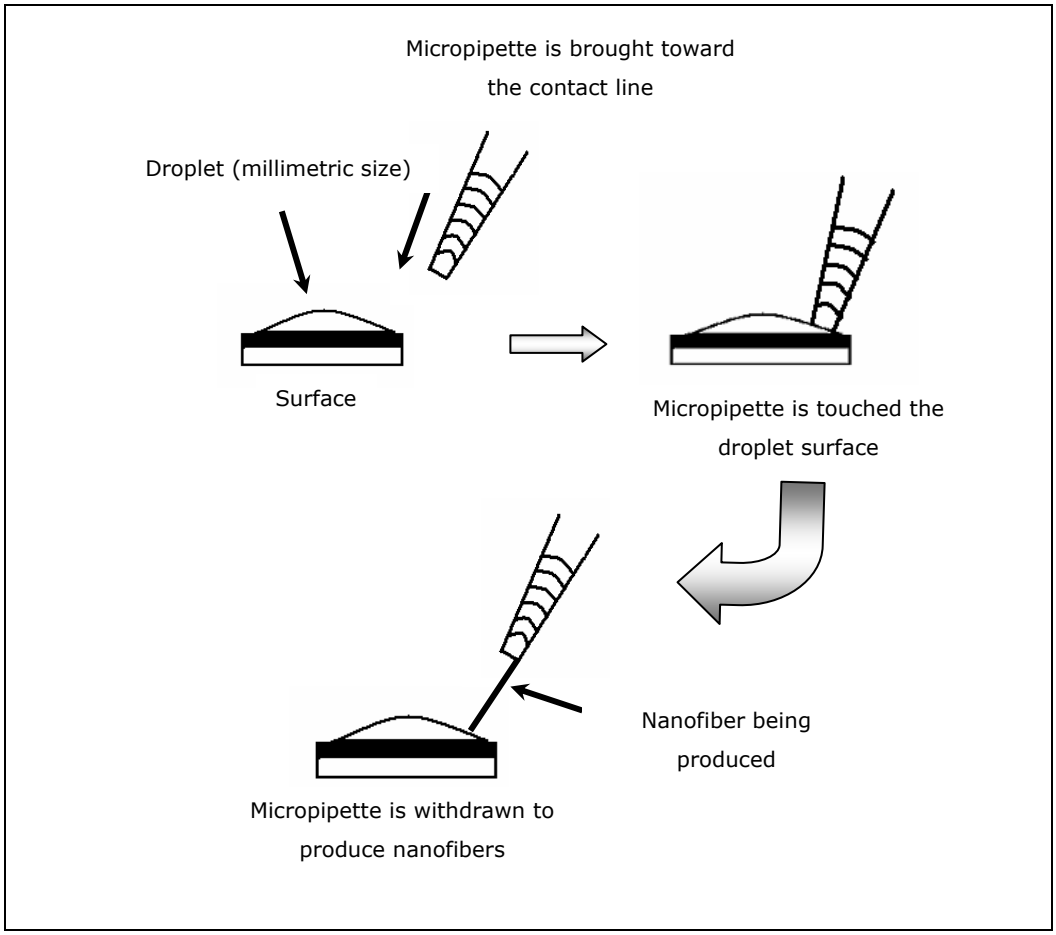

Figure 4. Nanofiber fabrication by drawing.

1.3.3. Template Synthesis

As the name implies, this method uses a nanoporous membrane as a mold or template to obtain the desired material or structure either in the form of solid nanofibers or hollow-shaped tubules. It is advantageous in that a variety of raw materials such as semiconductors, metals, polymers and carbons can be used in fiber fabrication. Feng *et al.* (2002) have used metal oxide as a template with nanoscale diameter pores [77]. Extrusion of the polymer solution through the porous membrane is achieved by water pressure. As soon as the polymer comes into contact with the solidifying solution, a fiber with diameter dependent on the template pore size is produced as shown in Figure 5.

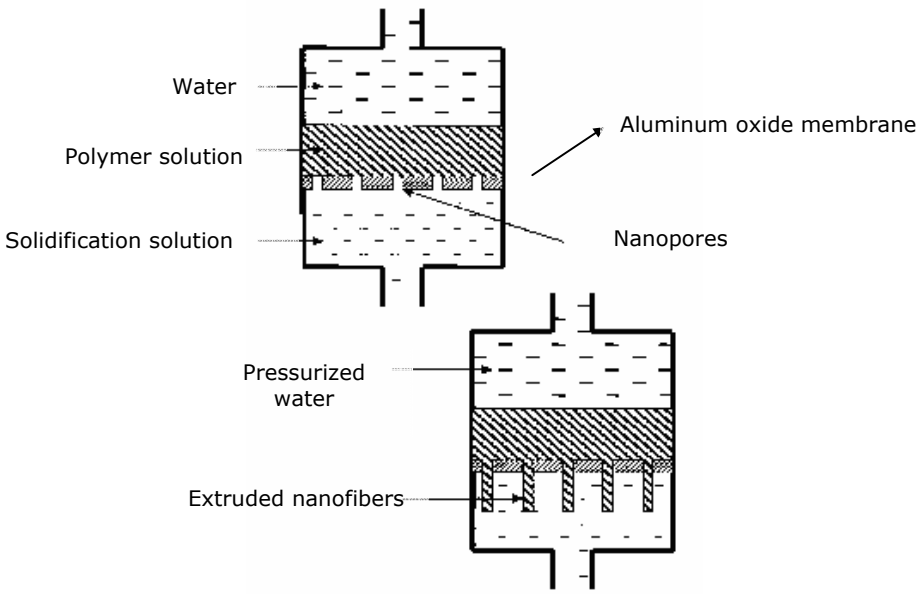

Figure 5. Nanofiber production by template synthesis [77].

The resultant fiber diameters vary from a few to hundreds nanometers. On the other hand, this method is limited in that nanofibers only a few micrometers long are obtained.

1.3.4. Phase Separation

This process has five steps, namely polymer dissolution, gelation, solvent extraction, freezing, and freeze-drying. First the polymer (preferably one that can gel) is dissolved in an appropriate solvent at the desired concentration. The solution is then stirred at a certain temperature (eg. 60 ºC for PLLA) for a period of time until a homogeneous solution is obtained. This is followed by transferring the solution into a refrigerator set to the gelation temperature of the polymer. The resultant gel is immersed in water several times to allow solvent exchange. Finally, the gel is removed from water, transferred to a freezer (-70^{o}C), and then the frozen gel is lyophilized [78]. A simple representation of this process is given in Figure 6, which shows how a nanoporous PLLA foam is produced.

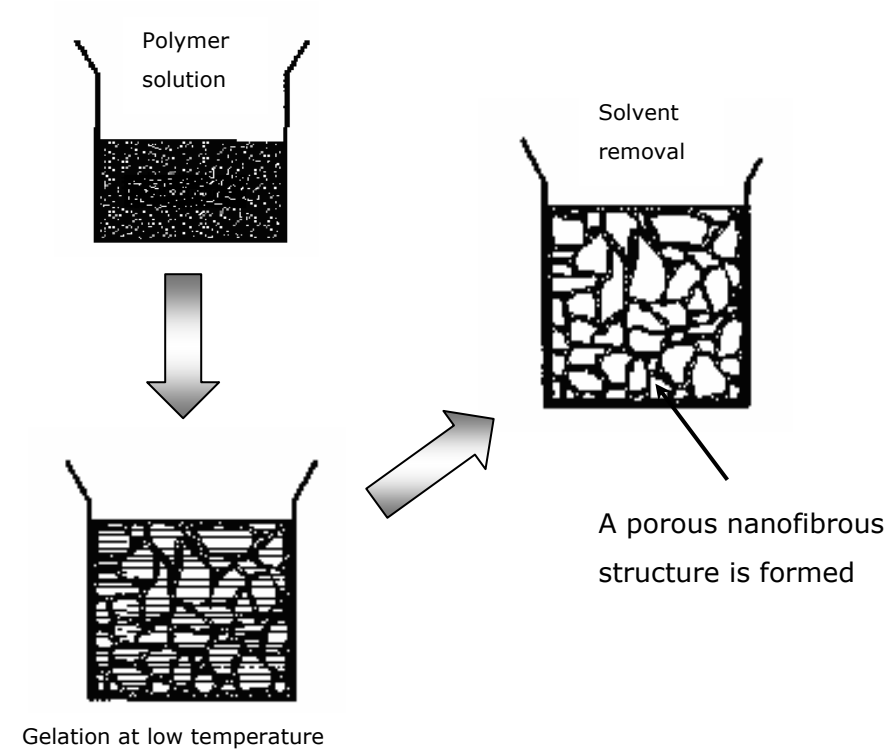

Figure 6. Nanofibrous structure production through phase separation.

In this process, phase separation occurs due to physical incompatibility and yields nanofibers, however, a long period is needed to transfer a solid polymer into a nano-porous foam. Fiber dimensions vary from 50 to 500 nm with a length of a few micrometers [16]. Therefore, the limitation of this method is that no long continuous fibers are produced and only the polymers that have gelation capability can be used to produce the nanofibrous structure.

1.3.5. Wet Spinning

This method is based on precipitation, where a polymer is drawn through a spinneret into a non-solvent. The process starts by dissolving the polymer in a suitable organic solvent or in a weak inorganic solvent in order to prepare the spinning dope (*Fig. 7*). The polymer solution with the desired concentration is transferred to a reservoir of a (glass) spinneret and the free end of the spinneret capillary is positioned in a bath containing a non solvent of the polymer. The solution is then allowed to flow under gravity through the spinneret into the non-solvent and precipitation or coagulation occurs. This results in fibers with a diameter range varying from 10 to 100 μm. Polymer solution concentration and the spinneret diameter are two crucial parameters that affect the resulting fiber properties. Fibers obtained by this process are in micro scale and are continuous.

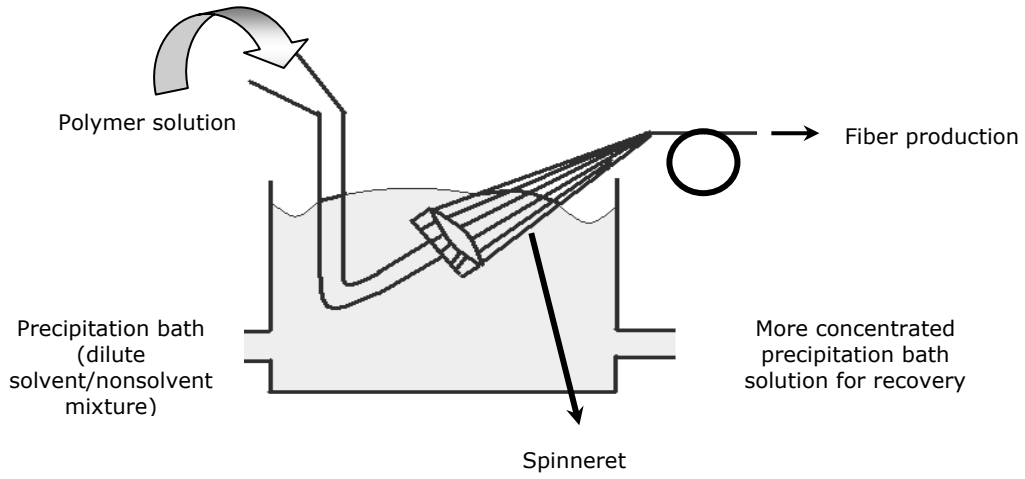

Figure 7. Wet spinning process.

This process has been tested in this study also in order to observe the effect of various micro-scaled fiber diameters on cell behavior such as attachment, proliferation and differentiation.

1.3.6. Electrospinning

The last and one of the most preferred methods of the last decade utilizes to produce fibers in nano and low microscale is electrospinning. The fundamental idea of this process dates back to more than 70 years ago; however the first 'eletrospinning' term was introduced in 1994. It was Formhals who first published a number of patents related to the set-up needed to produce polymeric filaments by means of electrostatic forces [79-83]. After that, only a few scientists continued their research on this process. Since 1980s and especially in the last 10 years there has been an increase in the attention paid by researchers to this method due to increase in interest in nanotechnology. The graph below presents the number of publications related to electrospinning in the last 7 years.

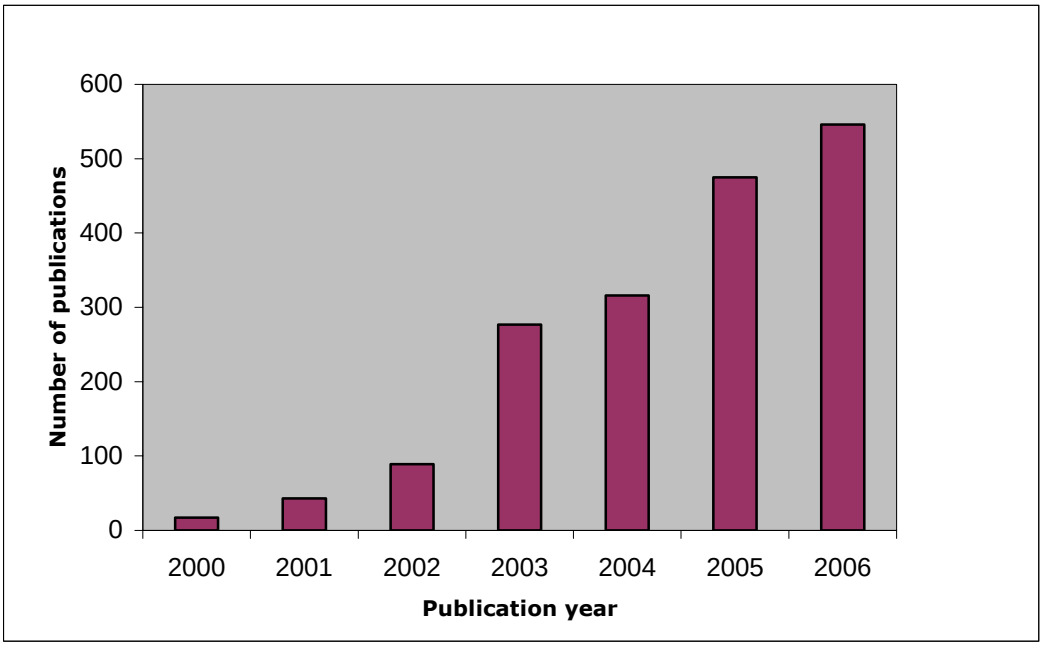

Figure 8. Increase in number of electrospinning-related publications from 2000 until now [SciFinder Scholar search system].

The main principle of this technique is the application of high electrostatic forces to draw (or eject) continuous filaments from a polymeric solution via a syringe [8, 39, 84, 85]. Basically, three components are necessary to accomplish the process; (1) a capillary tube ending in a needle of small diameter, (2) a high voltage supplier, and (3) a metallic collector. A more developed set-up could include a pump to achieve a certain polymer flow rate, a camera to record the process, and a controllable collector that can move in X, Y or Z directions (*Fig*. 10), even though there now exists a large number of sophisticated set-ups. As mentioned above, a high potential is used to produce an electrically charged jet of a polymer solution. One of the electrodes is connected to the needle that ejects the polymer solution whereas the other is connected to the collector.

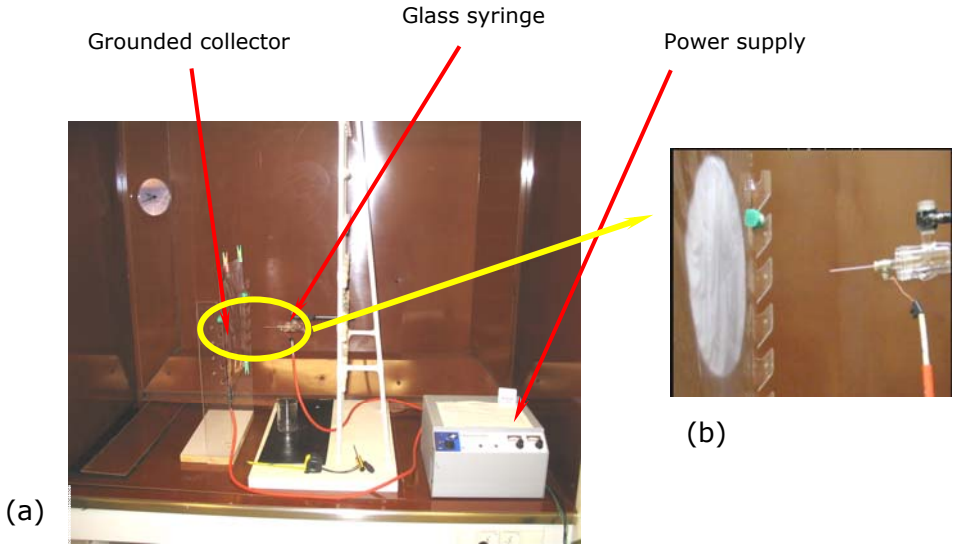

Figure 9. Electrospinning set up. (a) the system, and (b) in close up the fiber collection on a stationary, grounded plate collector.

The leakage of the polymer solution is initially prevented by surface tension; however, as the potential applied increases the contribution of surface tension starts to decrease due to charge repulsion and the shape of the fluid at the capillary tip changes from spherical to conical, which is known as Taylor cone [16, 65, 67, 86]. A further increase in the electric field leads the

repulsive electrostatic forces to overcome the surface tension of the solution. Meanwhile, the solvent evaporates and the charged jet of the solution is ejected from the capillary tip in the form of a long and thin fiber. Thus, fibers with varying diameters (depending on the polymer type and other process conditions used) are collected as a web of nano- and microfibers on the collector (*Fig. 9 b*), which can be either stationary or rotating (plate, cylinder or disc-shaped) (*Fig. 10*).

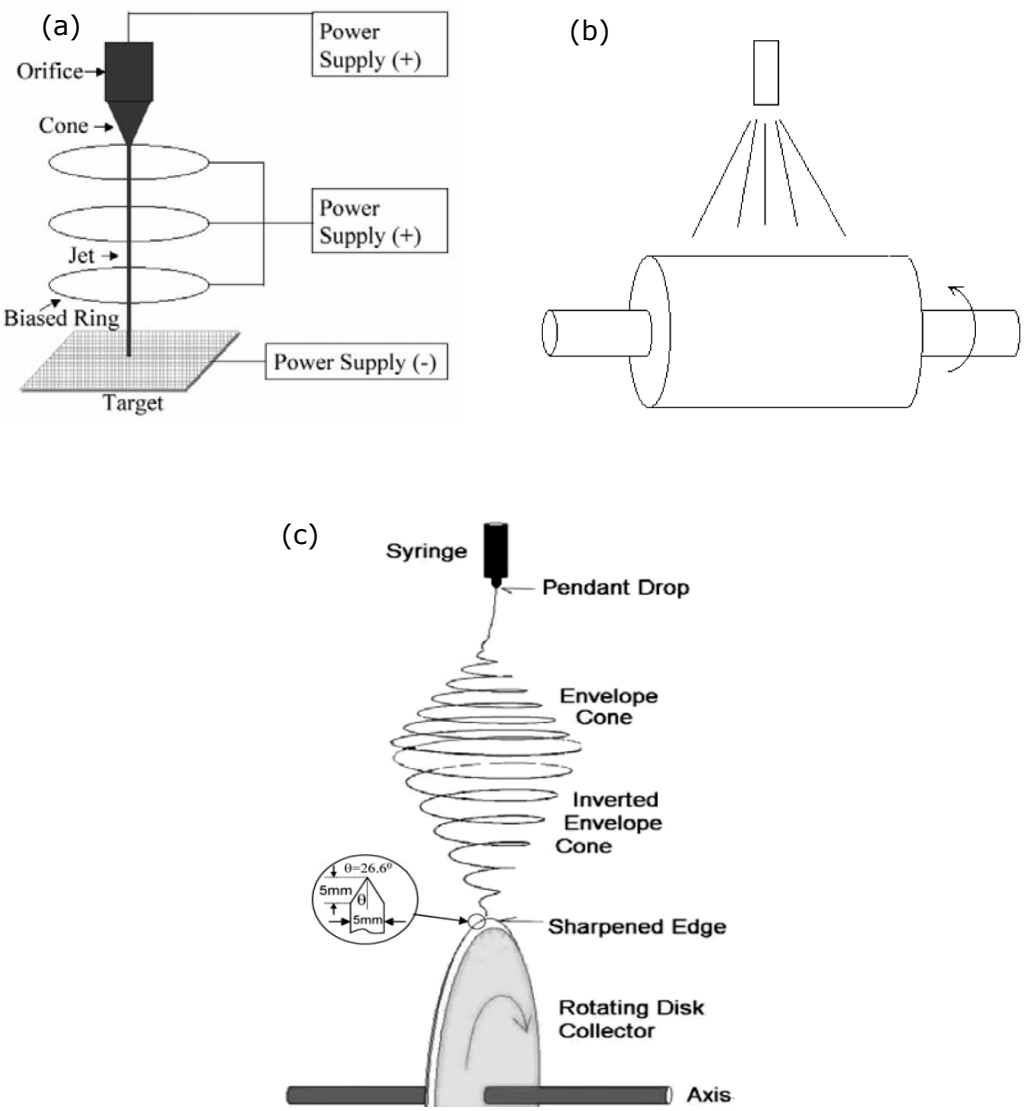

Figure 10. Different types of fiber collectors. (a) Plate type; (b) Cylinder type; (c) Disc type. [72]

The idea behind using various rotating collectors is to produce aligned nanofibers since they are more preferable in various fields such as electronics in the construction of photonic devices, or even in fiber-based reinforcements. With the use of this relatively straightforward and simple technique, more than 50 different types of organic polymers have been used to produce fibers with diameters ranging from tens of nanometers to a few micrometers [69, 72, 87].

Its simplicity, versatility, high control and reproducibility, ability to produce continuous fibers and the fact that it is more economical when compared to the other processes mentioned in the above sections has made electrospinning one of the most popular nanofiber-producing processes. Furthermore, electrospinning results in more continuous and thinner fibers and it produces fibers with diameters ranging from 3 nm to several micrometers. Self assembly, template synthesis and phase separation methods, on the other hand, produce fibers with diameters ranging from 500 nm to tens of micrometers and with only a few micrometers length [16].

1.4. Nanofiber Production Through Electrospinning

1.4.1. Parameters Affecting the Process

When a polymer is shown to be spinnable into nanofibers certain properties are targeted; fibers should be consistent, defect-free and have controllable diameters. To achieve these goals, a number of parameters need to be modified until optimization. The main parameters to control are the polymer type, its concentration, solvents, potential applied, distance between the needle tip and the collector, and the state of the collector [72]. Through these parameters fiber thickness, nano-mat porosity, pore size, surface chemistry and surface topography can be controlled [72, 88-90]. Optimization of the conditions in order to get the best results is a challenging task.

1.4.1.1. Process-Related Parameters

Potential has been found to be one of the most crucial parameters that affect electrospinning results [89-91]. For example, fiber morphology changes have been found to be correlated with the change in the applied potential. Electrospun PEO nanofibers were straight and defect-free at low potentials (5.5 kV), whereas at higher potentials the fibers had a high density of beads [89]. In contrast, increase in potential could also lead to a decrease in fiber diameter [88, 90]. Smaller sized beads and reduction in the number of beaded fibers were obtained when the potential was increased [88]. This is believed to be due to the whipping instability and resultant bead prevention is favored by high electric field applications. The current study also has shown that higher potentials give rise to thinner diameters even though the influence was not very significant above a certain voltage value. Pore size also has been reported to decrease with potential increase because the drawing rate and fiber crossings increase [88].

The hydrostatic pressure in the capillary tube of the needle can also affect the results. The polymer solution is forced out of the needle orifice by the applied electric field [92], gravity [87], or a pump [18, 93].

Zong *et al.* (2002) reported that lower volumetric feed rates result in smaller fiber diameters due to faster solvent evaporation [27]. However, Megelski *et al.* (2002) observed the opposite and showed that thicker electrospun polystyrene fibers are produced at higher flow rates [94]. Thus, even though a clear relationship between the flow rate and fiber diameter was not found, its influence on electrospun fiber properties is quite distinct.

The needle size has also been found to influence fiber diameter. Smaller needle orifices have been reported to contribute to thinner fiber formation [90].

The distance between needle and collector is another parameter. Short distances can be used when a highly volatile solvent is utilized. Solvents

with low vapor pressure, e.g. water, need longer distances to evaporate; otherwise, the fibers fuse. In addition, the distance has an effect on fiber morphology and diameter. Decrease in distance, regardless of the concentration of the polymer solution, results in the formation of wet fibers and beaded structures [93, 95]. Moreover, the shape of fibers changes from round to flat when the distance is decreased [95].

1.4.1.2. Environment-Related Parameters

Three main environment-related parameters that should be taken into consideration while processing are; solution temperature, medium humidity, and air velocity in the electrospinning chamber.

Increase in solution temperature results in solution chain formation, decrease in solution viscosity and increase in solvent evaporation. All these factors influence fiber morphology. For instance, Demir *et al.* (2002) reported that electrospinning of polyurethane at elevated temperatures resulted in a narrower diameter distribution compared to fibers electrospun at room temperature [96]. Their results also showed that it was possible to electrospin solutions with higher concentrations at elevated temperatures.

Casper *et al.* (2004) studied the influence of humidity and molecular weight on electrospun polystyrene fibers [97]. Increase in the molecular weight of polystyrene resulted in less uniform shaped but larger pores. On the other hand, it was found that an increase in humidity leads to an increase in diameter, number, shape and distribution of pores. A relative humidity higher than 30% led to micro- and nano-structured pores on the surface of fibers.

1.4.1.3. Polymer and Solvent-Related Parameters

Viscosity, elasticity, conductivity and surface tension of the solution are the most important and influential parameters. Appropriate solution viscosity is important for an efficient electrospinning process. At very low viscosities, the solution forms droplets, leading to what is called 'electrospraying'.

Electrospraying occurs, when entanglement of polymer chains does not occur but still undergoes a bending instability that causes a whip-like motion between the capillary tip and the grounded target. Very high viscosities, on the other hand, prevent ejection of the solution from the syringe tip due to a high surface tension and this is called suppression [23, 89, 98]. In addition to molecular weight and molecular weight distribution, other thermodynamic properties, e.g. crystallization and glass transition temperature also affect processing [94, 99]. The architecture of the polymer also affects processing; for instance, branched polymers seem to need a higher concentration than linear polymers in order to form defect-free nanofibers [100]. Studies revealed that increase in polymer concentration is accompanied by an increase in fiber diameter and decrease in bead formation [28, 90, 93, 94, 101, 102]. For example, poly(L-lactide) (PLLA) fiber diameter was found to increase with increasing polymer concentration, from 150-500 nm for 2% of PLLA concentration to 800–3000 nm for 5% of PLLA solution [25].

A highly volatile solvent is generally more preferable but this may change with the purpose of processing. Vapor pressure of the solvent is also very important. Chun *et al.* (2006) have investigated the effect of two different solvents (isopropyl alcohol and dimethylacetamide) on electrospinning of poly(ethylene-*co*-vinyl alcohol) [EVOH] and concluded that hydrogen bonding affects fiber diameter and morphology [91].

Effect of viscosity and surface tension of solvents have also been investigated. Piras *et al.* (2006) have used acetic acid and ethanol as solvents [102]. The more rapidly evaporating ethanol led to thicker nanofibers due to the lower surface tension of ethanol (22.4 dynes/cm) than that of acetic acid (28 dynes/cm). In addition, ethanol has a dielectric constant of 24.3 $C^2m^{-2}N^{-1}$ at 25°C, while for acetic acid it is 6.2 $C^2m^{-2}N^{-1}$ at 20°C. Lee *et al.* (2002) indicated that the electrolytic tendency of the solvent can be the most important parameter of electrospinning process [93]. It has been observed that addition of some salt (benzyl triethylammonium chloride (BTEAC)) to polymer solutions results in thinner fibers than those in solutions containing no salt [18]. This was explained as a result of an increase in the charge density, which brings more elongating

forces acting on the polymeric solution, and therefore, results in the formation of thinner and straighter fibers compared to the salt-free case. In some other studies, the drug diclofenac was used in its sodium salt form, diclofenac sodium (DS), and it was observed that addition of DS to the polymer dissolved in acetic acid gave rise to much thinner fibers [39, 102].

Consequently, the vapor pressure of the solvent should be suitable so that it evaporates quickly enough for the fiber to maintain its integrity when it reaches the target but not too quickly to allow the fiber to harden before it reaches the nanometer range. In addition to this, the viscosity and surface tension of the solvent must neither be too high to prevent the jet from forming nor be too low to allow the polymer solution to drain freely from the pipette.

1.5. Nanofibers in Tissue Engineering Applications

A rapidly growing field of application of polymer nanofibers is their use in tissue engineering. The main areas of intensive research are nerve [25], blood vessel [4, 27, 36, 56], skeletal muscle [37], cartilage [103, 104] bone [30, 105] and skin [106] tissue engineering. Most of the reports support that these nanofibrous structures are capable of supporting cell attachment and proliferation since the cells seeded on these scaffolds have shown to maintain their phenotypic shape and growth according to nanofiber orientation [107].

1.5.1. Nerve Tissue Engineering

Application of electrospun polymeric nanofibers for nerve tissue regeneration is quite new. Yang *et al.* (2005) investigated the efficacy of aligned PLLA nano-microfibrous scaffolds in nerve tissue engineering by utilizing neonatal cerebellum C17.2 stem cells [25]. The most important observation was the elongation and neurite growth of cells parallel to fiber direction, and the effect of fiber diameter was not so significant. They have found that aligned PLLA nanofibrous scaffolds are good scaffolds for neural tissue engineering.

1.5.2. Skin Tissue Engineering

Naturally derived polymer, chitin, was utilized by Noh and his coworkers (2006) in order to study the effect of electrospun chitin nano and microfibers and chitin microfibers (commercially available) on the behavior of human keratinocytes and fibroblasts [106]. The tested scaffolds were either modified by coating with collagen or unmodified. Nanofibers exhibited higher cell attachment and spreading, especially when coated with collagen than microfibers. These results proved the potential of electrospun nanofibers in wound healing and regeneration of skin and oral mucosa.

1.5.3. Blood Vessel Tissue Engineering

He *et al.* (2005) have investigated the behavior of human coronary artery endothelial cells (HCAECs) on P(LLA-CL) nanofibrous scaffolds modified with collagen [56]. Enhanced adhesion, spreading, viability and phenotype preservation of HCAECs was observed. Aligned PLLA-PCL nanofibers have also been tested for their suitability in blood vessel tissue engineering by other researchers [36]. Human coronary artery smooth muscle cells (HCASMCs) tested on the scaffold expressed a spindle-like phenotype aligned along the direction of nanofibers. Moreover, the attachment and proliferation rates of cells on fibrous scaffolds were observed to be significantly higher when compared to non-porous plane films of the same material. A number of other studies have shown that these biodegradable polymers mimic the natural ECM and show a defined structure replicating the *in vivo*-like vascular structures and can be ideal tools for blood vessel tissue engineering [4, 26].

1.5.4. Skeletal Muscle Tissue Engineering

Skeletal muscle is responsible for maintenance of structural contours of the body and control of movements. Extreme temperature, sharp traumas or

exposure to myotoxic agents are among the reasons of skeletal muscle injury. Tissue engineering is an attractive approach to overcome the problems related to autologous transfer of muscle tissue. It could also be a solution to donor shortage and reduction in surgery time. Degradable polyesterurethane membranes, either uncoated or coated with fibronectin and collagen were studied with three different cell types specific for muscle tissue; murine myoblast cell line (C2C12), rat myoblast cell line (L6), and primary human satellite cells (HSCs) [108]. The study demonstrated the absence of toxic residuals and satisfactory mechanical properties of the scaffold. All three cell types attached and proliferated on the scaffolds, showing the suitability of the material for skeletal muscle tissue engineering.

1.5.5. Cartilage Tissue Engineering

There are three forms of cartilage in the body that vary with respect to structure, chemical composition, mechanical property and phenotypic characteristics of the cells. These are hyaline cartilage, fibrocartilage and elastic cartilage. Cells capable of undergoing chondrogenic differentiation upon treatment with appropriate factors and a 3-D scaffold that provides a suitable environment for chondrogenic cell growth are the two main requirements for successful cartilage tissue engineering. In addition, there are some other conditions to fulfill. First, the matrix should support cartilage-specific matrix production; second, it should allow sufficient cell migration to achieve a good bonding to the adjacent host tissue and finally, the matrix should provide enough mechanical support in order to allow early mobilization of the treated joint [109]. Mesenchymal stem cells and chondrocytes are the two main cell types for cartilage tissue engineering. Wang *et al.* (2006) investigated the suitability of silk fibroin scaffolds in the promotion of growth of adult human chondrocytes, and therefore, new cartilage formation [103]. The cells seeded on the silk fibroin scaffolds were observed to regain the spherical morphology similar to that in the natural environment. Cell redifferentiation by the up-regulation of cartilage-related gene transcripts also occurred. Thus, this combination was concluded to be suitable for engineering a cartilage tissue.

1.5.6. Bone Tissue Engineering

Bone engineering has been studied for a long time to repair fractures and in the last decades, used in preparation of dental and orthopedic devices and bone substitutes. Bone tissue engineering is a more novel technique, which deals with bone restoration or augmentation. The matrix of bone is populated by osteogenic cells, derived of mesenchymal or stromal stem cells that differentiate into active osteoblasts. Several studies have demonstrated that it is possible to culture osteogenic cells on 3-D scaffolds and achieve the formation of bone. Tuzlakoglu *et al.* (2005) has tested bone tissue engineering with starch/PCL-based carriers [10]. They designed a novel 3-D carrier composed of micro and nanofibers and have observed that cells used these nanofibers as bridges to connect to each other and to the microfibers. Furthermore, a higher ability for enhancement of cell attachment and a higher alkaline phosphatase activity was observed in the nano/microfiber combined scaffolds compared to the microfibrous carrier.

Fibrous silk fibroin scaffolds containing bone morphogenetic protein 2 (BMP-2) and/or nanoparticles of hydroxyapatite (nHAP) were tested with human bone marrow-derived mesenchymal stem cells (hMSCs) [4]. The scaffolds with BMP-2 supported higher calcium deposition and had enhanced transcript levels of bone-related specific markers. Addition of nHAP to the fibrous scaffolds improved bone formation. The best result was obtained when both BMP-2 and nHAP existed together.

1.6. Cell Sources Used in Tissue Engineering

Cells used in tissue engineering applications come from three sources: (1) *autologous* cells taken from the patient's own cells; (2) *allogenic* that are expanded from another person's tissue, and (3) *xenogenic* cells taken from a different species. Since no inflammation and no body reaction to foreign bodies is desired the first source is the most preferable. The use of the other two types of cells requires special care. The utilization of embryonic or adult

stem cells is an exciting new possibility because these could be induced to differentiate into a range of cell types after manipulation with chemical and biological factors. This is especially helpful in cases where sufficient cell isolation is difficult. The decision to use primary or stem cells mainly depends on the proliferative ability of the cell type. Keratinocytes, osteoblasts and chondrocytes can be isolated and expanded from a small biopsy at a reasonably fast rate. This, however, is not the case for all cell types. In some cases expansion can cause dedifferentiation and use of embryonic stem cells can solve this problem since they both have a high self-renewal capacity and a potential for directed differentiation [110]. There are certain social and ethical issues concerning the use of embryonic stem cells in tissue engineering and this can partially be overcome by the use of adult stem cells.

Several studies have been carried out to study cell behavior on electrospun, nanofibrous scaffolds. Cell viability, attachment, proliferation and differentiation were the most important parameters studied. Some of the cell types used include keratinocytes [13], hepatocytes [43], endothelial cells [6, 26, 29, 37, 38, 111], myoblasts [108], satellite cells [108], smooth muscle cells [7, 37, 38, 42, 49, 57], myofibroblasts [92], ligament fibroblasts [112], articular chondrocytes [51], osteoblasts [15, 25, 51], mesenchymal stem cells [30, 35, 47], and fibroblasts [13, 35, 42, 45, 67].

1.7. Surface Modification

Surface modifications also attracted attention of many researchers because cell behavior on polymer substrates is often governed especially by the surface characteristics, such as chemical composition, ionic charge, wettability, texture and topography [114]. Ideal biomaterials provide proper cell-substrate interaction and stimulate the cells by substrate-bound chemical, biological, electrical and mechanical signals. In many cases, polymeric materials are subjected to surface modification or functionalization if the bulk properties of the material are suitable for the construction of a tissue-engineering scaffold and if the surface properties are not. For instance, surface hydrophobicity or hydrophilicity of the material may be

altered [115]. Attachment of molecules such as those containing RGD sequences are expected to modify the surface of the scaffold and result in improvement of cell adhesion. Some other modifications of the surface could be through attachment of functional groups or creation of some 2D and 3D patterns on the surface so that cell alignment is guided and new tissue formation is improved. Surface modification methods can be classified in three groups namely, physical (physical adsorption, Langmuir-Blodgett film), chemical (oxidation by strong acids, ozone treatment, chemisorption and flame treatment) and radiation (glow discharge, corona discharge, photo activation (UV), laser, ion beam, electron beam and γ-irradiation).

Plasma surface modification has been utilized in this study in order to improve the hydrophilicity of PHBV material used. Adhesion promotion, enhanced surface wettability, improvement of biocompatibility, and surface functionalization are some of the advantages offered by this method. The working principle of this technique is the creation of glow discharge plasma (after evacuating a vessel and then refilling it with a low-pressure gas) and then energizing the gas by microwaves, alternating current, direct current or radio frequency energy techniques. The surface of the sample placed in this chamber is bombarded with these energetic species (ions, electrons, radicals, photons) and the energy transferred leads to some chemical and physical processes such as etching, crosslinking, bond breakage, deposition, and functionalization, all of which result in surface modification. The main parameters that affect the process are processing conditions such as the applied power, gas type, duration, operating pressure and system properties such as electrode location, reactor design, gas inlets and vacuum [115].

1.8. Summary of the Used System

The aim of this study was to evaluate the influence of fiber size of fibrous tissue engineering scaffolds on cell behavior (attachment, proliferation and differentiation). Two main fiber-processing methods were chosen to obtain the desired fibrous scaffolds with varying diameters. Wet spinning was utilized to obtain fibers with micrometer scale diameters. In general, the diameters obtained by this method are in the 10-100 μm range.

Electrospinning technique was chosen as the nanofiber production method. One of the most important advantages of using this technique is that the resulting fibers are in nanoscale, meaning that this fine fibrous scaffold possesses a high surface area to volume ratio and a good environment for adhesion and growth of cells. In addition, their nanosized pores and pore interconnectivity, the flexibility of electrospun nanofibers in surface functionalities and their better mechanical performance (stiffness, tensile strength, etc.) are important advantages of this method. Based on these evaluations, this technique was also used in the current study and the influence of parameters such as fiber diameter, surface porosity of the scaffolds, polymer type and plasma modification on cell attachment and behavior were studied.

Choice of an appropriate polymer type was also important to perform this study. In the present case, PHBV, the simplest and most extensively studied biological polyester, a polyhydroxyalkanoate (PHA) *(Fig. 11)*, was used since it is considered to be a good candidate for tissue engineering applications [19, 21, 22, 63]. PHBV was utilized as pure or with some polylactides as blends with a 1:1 ratio.

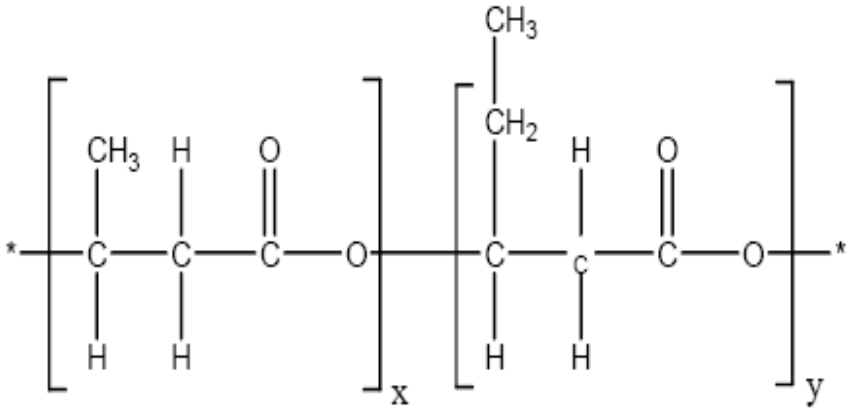

Figure 11. Poly(3-hydroxyalkanoate) (P3HA).

CHAPTER 2

MATERIALS AND METHODS

2.1. Materials

Poly(3-hydroxybutyrate-co-3-hydroxyvalerate) (PHBV), containing 8 % hydroxyvalerate, was purchased from Sigma-Aldrich Co. (USA). PLLA, P(L,DL)LA (70:30), PLGA (75:25) and PLGA (50:50) were purchased from Boehringer-Ingelheim (Germany). Chloroform and N,N-dimethyl formamide (DMF) were obtained from Merck (Germany).

Newborn calf serum, Amphothericin B, trypsin/EDTA, cacodylic acid (sodium salt) and DAPI were purchased from Sigma-Aldrich Corporation (Germany). Acridine Orange was obtained from BDH Chemicals Ltd. (UK). Fetal calf serum and Dulbecco's Modified Eagle Medium (DMEM; low glucose) were from PAA (Austria). Dulbecco's Modified Eagle Medium (DMEM; high glucose) was supplied by Gibco (USA). Formaldehyde, acetic acid, sodium dihydrogen phosphate, and disodium hydrogen phosphate were obtained from Merck (Germany). NucleoCounter reagents were purchased from Chemometec (Denmark) and MTS cell proliferation assay solution was obtained from Promega (USA).

2.1.1 Cells

Human osteosarcoma cells (primary culture) (SaOs-2) were provided from ATCC and Dr. Karine Anselme (Institut de Chimie des Surfaces et des

Interfaces, Mulhouse, France). All the cells were stored in a liquid nitrogen tank. SaOs-2 with passages between 12-16 were used in the experiments.

2.2. Methods

2.2.1. Nano/microfibrous scaffold preparation

Two methods, electrospinning and wet spinning, were utilized in the production of the nanofibers and microfibers, respectively.

2.2.1.1. Wet spinning

PHBV solutions (5, 10, 15 and 20% (w/v)) in chloroform were prepared and extruded through a syringe into a non-solvent miscible with the polymer (methanol). As soon as the polymer solution was introduced to the non-solvent while stirring at an appropriate rate, the microfibers formed. The liquid phase was discarded and the resulting fibers were freeze-dried in order to dry the fibers. This procedure was optimized by changing some of the parameters that influence fiber diameter. Two main parameters that were varied were the polymer solution concentration and stirring rate. For instance, the concentration was kept constant (eg. 5 % (w/v)) and the stirring rates of the non-solvent was varied from 600 rpm to 1200 rpm. In another series, the stirring rate was kept constant (eg. 600 rpm) and the polymer concentration was varied between 5 to 20 % (w/v) (Table 3).

2.2.1.2. Electrospinning

Nanofibers were obtained by electrospinning process. The electrospinning set up utilized in this study consisted of a high voltage supply (Chargemaster, SIMCO Co., USA), a 2 mL syringe capped with a 22 Ga (with an inner diameter of 0.644 mm) needle and a copper, grounded collector *(Fig. 9)*.

PHBV and four of its blends (PHBV-PLLA, PHBV-P(L,DL)LA (70:30), PHBV-PLGA (75:25) and PHBV-PLGA (50:50)) were used. Influence of process parameters and presence of benzyl triethyl ammonium salt on fiber properties were investigated (Table 4).

2.2.1.2.1. Electrospinning pure PHBV solutions

The polymer concentrations were 5% - 9%, 15% and 20% (w/v) (Table 4) in solvents chloroform or chloroform:DMF 96:4 (v/v). Electrospinning was carried out using 10 or 30 mm long, 22 Gauge needles. The positive electrode was connected to the metallic needle attached to the end of the syringe and, thus, the polymer solution was positively charged. The negative (target) electrode was located 20 or 30 cm away from the tip of needle. An aluminum foil, on which the sample was collected, was placed over this copper counter electrode. The applied potential was varied in the range 20–50 kV.

The experimental electrospinning parameters were adjusted until a good Taylor cone shape and a continuous thin polymer jet were obtained. The influence of the parameters on fiber diameter was also studied. Initially, the polymer concentration (i.e. 5%) and the potential (i.e. 20 kV) were kept constant and the distance was changed (from 20 to 30 cm). Then, concentration and distance were kept constant (5% (w/v) and 30 cm) and the potential was varied (20, 30 and 50 kV). The same procedure was applied to all other polymer concentrations.

2.2.1.2.2. Electrospinning PHBV blends

Four different 1:1 (w/w) blends, namely, PHBV-PLLA, PHBV-P(L,DL)LA (70:30), PHBV-PLGA (75:25), and PHBV-PLGA (50:50) were tested. The first two blends were tested as 5% (w/v) solutions in $CHCl_3$-DMF (96:4) whereas the other two were 15% (w/v) solutions again in the same solvent. The distance, the potential and the needle length were set as 35 cm, 30 kV and 10 mm, respectively.

2.2.1.2.3. Electrospinning to obtain aligned PHBV and PHBV blend fibers

10 and 15% PHBV8 and 5% PHBV8-PLLA, 5% PHBV8-P(L,DL)LA (70:30), 15% PHBV8-PLGA (50:50) 1:1 (w/w) blend solutions were used. The solvent was $CHCl_3$-DMF (96:4) mixture. The process parameters were set as 25 cm distance, 20 kV potential and 10 mm needle length. In this case, the obtained fibers were collected not on a stationary collector but over a rotating copper collector, which was in cylindrical form with a diameter of 2 cm and the speed of rotation was adjusted to 2000 rpm.

2.2.2. Characterization of the scaffolds

In order to examine the electrospun nanomat structure, scanning electron microscope (SEM) was used. Samples were sputter coated with gold (Edwards S150 sputter coater) and viewed using a JEOL T100 (JEOL Ltd., Tokyo, Japan) microscope. Fiber diameter and bead dimensions (length and diameter) were measured in 3 random fields by means of Image J 1.33u program (NIH, USA). The average size of fibers was measured using SEM micrographs with 2000 and 5000 fold magnifications. The image of each sample was divided into four regions by applying a grid and the mean diameter of fibers was calculated using the results of 25-30 measurements from three randomly selected fields.

All the cell seeded samples were examined by SEM (JSM 6400, JEOL, Japan). Before examination, the scaffolds were rinsed thoroughly with cacodylate buffer (pH 7.4), lyophilized, and gold coated under vacuum with a sputter coating device (Hummle VII, Anatech, USA).

2.2.3. Surface modification of the scaffolds

Oxygen plasma treatment (Advanced Plasma Systems Inc., USA) was carried out in order to improve the hydrophilicity of fiber surfaces. The instrument used in this study was composed of a vacuum chamber, a manifold unit, a vacuum pump, a power distribution box, a radio frequency (RF) power supply and a matching network (*Fig. 12*).

The main parameters that affect the degree of treatment are gas composition, exposure time, (RF power, and chamber pressure. Fibrous mat samples were treated exposing the one side facing the RF oxygen plasma reactor (Advanced Plasma Systems Inc., USA). They were placed in the plasma reactor chamber in a petri dish and the chamber was first evacuated. Then the chamber was filled with oxygen at very low pressures. Exposure time and RF power were set to be 5 min and 50 W, respectively.

Figure 12. Plasma treatment instrument.

2.2.4. Measurement of Surface Porosity of Scaffolds

The porosity of the upper surface of the scaffolds was assessed from the SEM micrographs (JEOL JSM 6400, JEOL Ltd., Japan) by means of NIH Scion Image program.

2.2.5. *In vitro* Studies

2.2.5.1. SaOs-2 Cell Culture

SaOs-2 human osteosarcoma cells were at passage 12 and propagated until passage 16. The medium composition for 500 mL was as follows: 448 mL of DMEM high glucose, 50 mL of fetal calf serum, 2 mL amphotericin B (1 µg/mL) and 200 µL antibiotic composed of streptomycin (100 µg/mL) and penicillin (100 UI/mL).

Cells were stored frozen, with their appropriate medium and 15% DMSO, in a liquid nitrogen tank at -196°C. Following thawing, the cells were used after reaching confluency. During cell culturing the cells were incubated in a CO_2 incubator (Sanyo MCO-17 AIC, Sanyo Electric Co. Ltd., JAPAN) at 5% CO_2 and 37°C. The in vitro experiments were conducted under standard culture conditions.

2.2.5.2 Cell Seeding onto Scaffolds

The medium was discarded from the flask, the cells were detached with Trypsin (0.25%)-EDTA treatment for 5 min at 37°C. After detachment, trypsin was deactivated with serum and the cells were collected by centrifugation at 3000 rpm for 5 min. The supernatant was discarded and the cell pellet was resuspended in 3 mL fresh medium. After that, the cells were counted with a Nucleocounter (Chemometec A/S Nucleo Counter, DENMARK). After determining the live cells, 30 µL of SaOs-2 containing medium was seeded onto a fibrous sample to create a cell density of $5x10^4$

cells/cm^2. The scaffolds were then incubated in the CO_2 incubator for 150 min in order to allow the cells to attach on the scaffold. Finally, 1 mL of medium was added into each well.

2.2.5.3 Cell Proliferation on Scaffolds

Cell Titer 96™ non-radioactivity Cell Proliferation (MTS) assay (1 mL, 10% in DMEM low glucose medium) was used to determine the cell density inside the polymer scaffolds. SaOs-2 seeded fibers were transferred into a new, sterile 24-well plate and washed with sterile PBS for many times in order to remove any remaining medium. 500 µL of MTS/PMS reagent was added to each sample in the 24-well plate and incubated for 2 h at 37ºC in a CO_2 incubator (all experiments were performed in triplicate). After 2 h of incubation, 100 µL of solution from each carrier well was transferred in triplicate to a new 96-well plate. Absorbance was determined at 490 nm using an Elisa Plate Reader (Molecular Devices, Model Maxline, USA). This test was performed on Day 1, 7 and 14 after seeding. A calibration curve of Cell Numbers vs Absorbance was constructed (Appendix A).

2.2.5.4. Fluorescence Microscopy

Fluorescence microscope (Olympus IX 70, Japan) was utilized to study the effect of texture and surface chemistry on cell morphology and cytoskeleton organization. Cells were seeded on the polymeric fibers as was described above. At the end of 1^{st}, 7^{th} and 14^{th} days the samples were prepared for microscopic observation and studied. The staining procedures are given in the following sections.

2.2.5.4.1. DAPI Staining

Some of the fibrous samples were stained with nuclear DAPI stain. After fixation in 3.7% formaldehyde solution for 30 min, specimens were rinsed with PBS and then DAPI solution (diluted 1:1000 in PBS solution) was applied onto the scaffolds which were then incubated at 37°C in dark for 45

min. Afterwards, specimens were rinsed with PBS and examined using an Olympus IX-70 fluorescence microscope with WU filter (330-385 nm).

2.2.5.4.2. FITC-Labeled Phalloidin Staining

FITC-labeled phalloidin staining was performed in order to observe the orientation of SaOs-2 cytoskeletal actin filaments. Samples were fixed with 3.7% formaldehyde for 30 min and then washed with PBS (pH 7.4). Cell membranes were permeabilized with a 1% Triton X-100 solution for 5 min at room temperature. After washing with PBS, samples were incubated at 37 °C for 30 min in 1% BSA containing PBS solution in order to block the non-specific binding sites. After washing, FITC labeled phalloidin (1:100 dilution in 0.1% PBS-BSA) was added and samples were incubated for another 1 h. Finally, the samples were washed with 1% PBS-BSA solution, transferred to a microscope slide, covered with 50% PBS-glycerol and observed using an Olympus IX-70 (Japan) fluorescence microscope. WB filter with a wavelength range of 450-480 nm was used for the observation.

2.2.5.4.3. Double Staining (FITC-Labeled Phalloidin and DAPI)

The procedure utilized was described in the previous sections but in this case the fibrous samples were stained with both DAPI and FITC-labelled Phalloidin at the same time. The stained cells were examined with the filters described above.

2.2.5.4.4. Acridine Orange Staining

SaOs-2 seeded fibers were washed with PBS (10 mM, pH 7.2) and fixed after 1, 7, and 14 days with 3.7% formaldehyde for 30 min at room temperature. The samples were washed with 0.1 M PBS. Hydrochloric acid (1 mL of 0.1 M) was added over each fiber sample, and then discarded after 1 min. One mL of 10% Acridine Orange was added and maintained for 15 min and meanwhile the specimens were protected from light exposure by covering the plate with an aluminum foil. The samples were then rinsed

several times with distilled water and observed using Olympus IX-70 fluorescence microscope by WB filter in the range of 450-480 nm.

2.2.5.5. Confocal Laser Scanning Microscopy (CLSM)

Confocal microscopy (Zeiss LSM 9100, Germany) was used to assess the distribution of cells within the fibrous structure of the scaffolds. Specimens were stained with 10% Acridine Orange and FITC-labelled Phalloidin in the same way as described above. An argon laser was used to excite the dyes and examine the specimens.

2.2.5.6. SEM Examination

Osteosarcoma seeded fibers were fixed after 7 and 14 days with 2.5% glutaraldehyde in 0.1M, pH 7.4 sodium cacodylate buffer for 2 h and then washed well with cacodylate buffer and distilled water several times. After that, all the fibers were sputter coated with gold and studied with a scanning electron microscope.

2.2.7. Statistical Analysis

Statistical analysis was carried out by the Student's t-test; $p \leq 0.05$ was considered to be significant.

CHAPTER 3

RESULTS AND DISCUSSION

3.1 Nano/microfibrous scaffold characterization

Before starting the *in vitro* experiments; the physical characteristics of scaffolds that affect cellular behavior, such as fiber thickness and shape, scaffold surface porosity of both wet spun and electrospun scaffolds and the effect of plasma treatment on the electrospun ones were investigated.

3.1.1. Wet spun fibers

The most important parameters that influenced the diameter of fibers were polymer concentration and stirring rate of the non-solvent (methanol). Four different polymer concentrations, namely 5, 10, 15 and 25% (w/v), were tried. It was observed that the diameter of fibers decreased with decrease in polymer concentration (*Fig*. 13).

However, there was a problem with the continuity of the fibers because the fibers produced at low concentrations such as 5 and 10% (w/v) were short, even though the diameter was reduced. Too high concentrations (20%) resulted in fibers with large diameters and the process became more difficult due to the high solution viscosity. The best results were obtained with 15% (w/v) solutions and the diameter obtained was in the 10-25 μm range (*Table 3*).

A second parameter that influenced the fiber diameter was the stirring rate of the non-solvent. The results obtained revealed that the higher the stirring rate, the smaller the resultant fiber diameter (*Table 3*), but at very high

stirring rates the continuity of the fibers decreased (data not shown). As a consequence, optimization of the stirring rate was necessary. Microfibrous scaffold surface porosity was not measured for these samples but it was observed that it was higher compared to that of electrospun nanofibrous scaffolds.

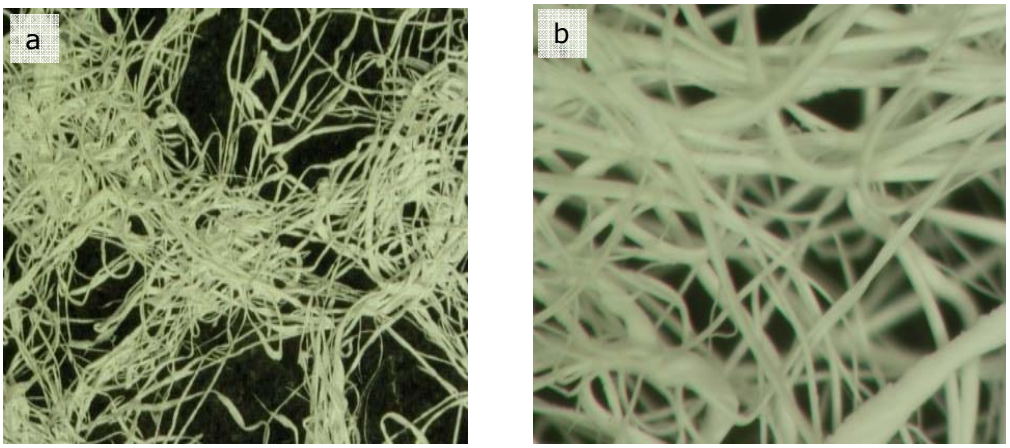

Figure 13. Wet spun fibers obtained using (a) 5% (w/v) and (b) 15% (w/v) PHBV in chloroform. Original magnification: x 40.

Table 3. Effect of polymer concentration and stirring rate on fiber diameter.

	Fiber Diameter (μm)		
Concentration % (w/v)	Stirring rate (rpm)		
	600	900	1200
5	50	25	10
10	30	20	10
15	25	15	10
20	40	30	25

Wet spun fibers were tested *in vitro* using human osteosarcoma SaOs-2 cells to investigate their suitability as carriers for bone tissue engineering. The cells did not prefer these fibers as a scaffold; Acridine orange staining revealed that the cells stayed round and did not spread (*Fig. 14*). Cell

behavior and morphology was observed by Moroni *et al* (2006) to be different on fibers with and without nanopores where cells spread well or just aggregated in round shapes, respectively [116], and this was explained to be due to the effect of radius of curvature of single fibers. Since fibers with larger diameters offer lower curvatures, cells prefer aggregating and staying non-spread and round shaped over the fiber surfaces. However, fibers with diameters close to cell dimensions lead to higher number and well spread cells since the effect of curvature is less predominant in this case.

In this part of the study cell behavior on wet spun fibrous scaffolds was not satisfactory, and therefore, they were not tested further for potential bone tissue engineering applications.

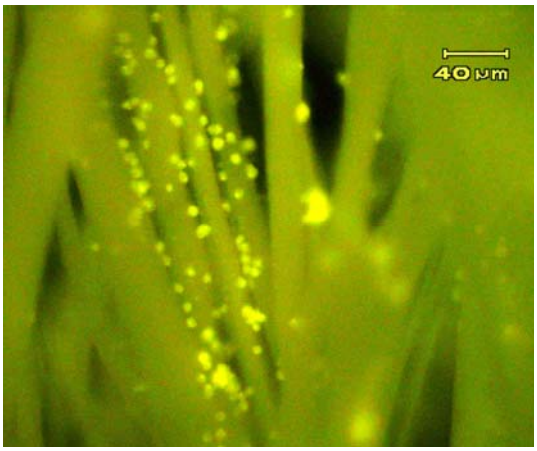

Figure 14. Fluorescence micrograph of Acridine Orange stained human osteosarcoma SaOs-2 cells on wet spun 15% PHBV fibers (stirring rate: 900 rpm).

3.1.2. Electrospun fibers

3.1.2.1. Influence of Polymer Concentration on Nanofiber Properties

PHBV solutions in chloroform (5-9%, 15%, 20%, (w/v)) were used to investigate the effect of polymer concentration, or solution viscosity, on

nanofiber properties. The ejected material was in the form of a single fiber rather than a multiple jet. Solutions with high concentrations (such as 20 %) were very difficult to electrospin most probably because the surface tension prevented the solution from being ejected. Very dilute solutions were also not suitable because then fiber fusion occurred due to the presence of large amounts of solvent in the electrospun fibers. Also with dilute solutions bead occurrence was more common. Beads are known to form as a result of high instability in the polymer jet. Three main factors, namely, surface tension, solution viscosity and charge density are influential on this phenomenon [13, 116]. Upon increasing the polymer concentration (from 5% to 15 %(w/v)) bead shapes were observed to change from spherical to spindle-like and upon further increase only fibers without beads were obtained *(Fig. 15)*.

The change in bead shape can be attributed to the competition between solution viscosity and surface tension. At low concentration, and therefore, low viscosity, surface tension overcomes the viscoelastic forces and the bead formation is more common.

The opposite occurs at high concentrations where viscoelastic forces are more influential than surface tension and beads are eliminated completely [102]. In addition to bead disappearance, fiber diameter was also found to increase with increasing polymer concentrations; 284 ± 133 nm with 5% PHBV in $CHCl_3$ and 2200 ± 716 nm when the concentration was 15% *(Table 4)*. Nonuniform fiber formation was also observed in the high concentration polymer solutions (Figure 15 c). The optimal concentrations were found to be in the range of 10 – 15 % (w/v) where both bead formation was absent and more straight and more uniform thickness fibers were obtained *(Table 4)*.

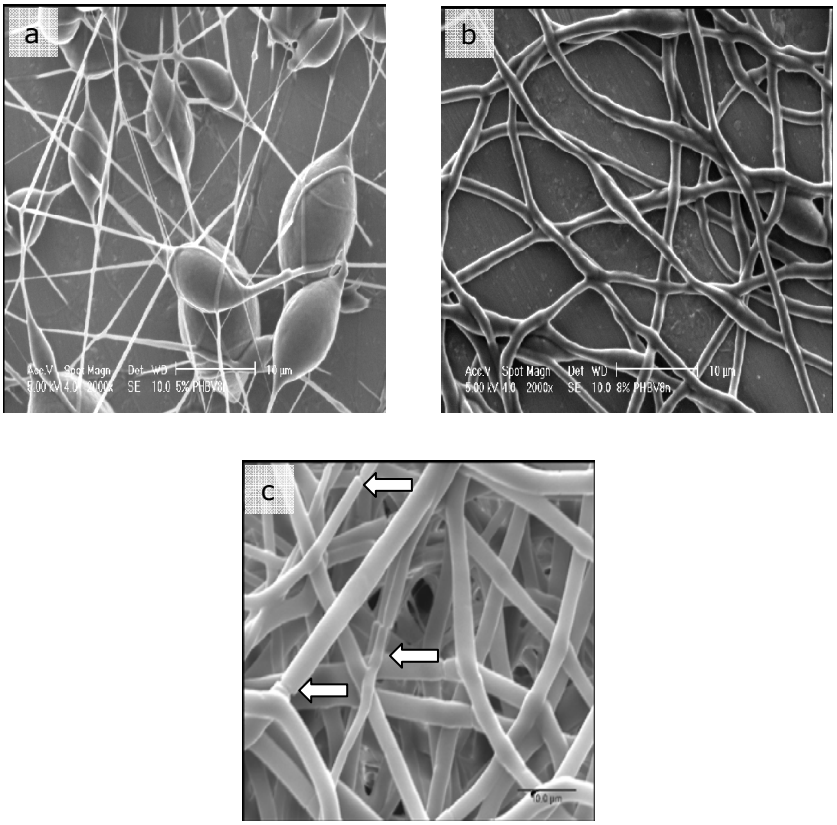

Figure 15. Effect of polymer concentration on fiber diameter and bead shape (PHBV in chloroform) (a) 5 % (w/v), (b) 8% (w/v) and (c) 15 % (w/v) (original magnification: x2000). Arrows indicate nonuniformity or kinks.

Table 4. Influence of concentration and polymer type on fiber diameter.

SAMPLE	(%) (w/v)	BTEAC SALT (2% w/w)	SOLVENT	D (nm)	COMMENT
PHBV	5	-	$CHCl_3$	284±133	Beads
	8	-		639±241	Beads
	9	-		733±322	Less beads
	15	-		2200±716	No beads but not homogeneous fiber diameters
	7	+		622±230	No beads but fusion
	10	+		823±322	No beads, less fusion
	15	+		1254±355	No beads, less fusion
	7	-	$CHCl_3$+DMF (96:4)	723±260	No beads, fusion
	10	-		862±296	No beads, fusion
	15	-		1166±248	No beads, no fusion
PHBV-P(L,DL)LA (70:30)*	5	-		1509±283	No beads, straight fibers
PHBV-PLLA*	5	-		377±97	Some beads but good fibers
PHBV-PLGA (50:50)*	15	-		1176±289	Some spindle-like beads
PHBV-PLGA (75:25)*	15	-		978±377	Too many beads, not a good fiber structure

*All blend ratios are 1:1; D: Average fiber diameter

3.1.2.2. Effect of Potential on Fiber Properties

In the study, potential was varied between 20 and 50 kV while the distance between the syringe tip and collector and the polymer concentration were kept constant at 30 cm and 8 % (w/v), respectively. It was observed that an increase in potential did not significantly affect fiber diameter (850 ± 181 nm for 20 kV; 785 ± 318 nm for 30 kV; 720 ± 151 nm for 50 kV) but bead formation was reduced *(Fig. 16)*.

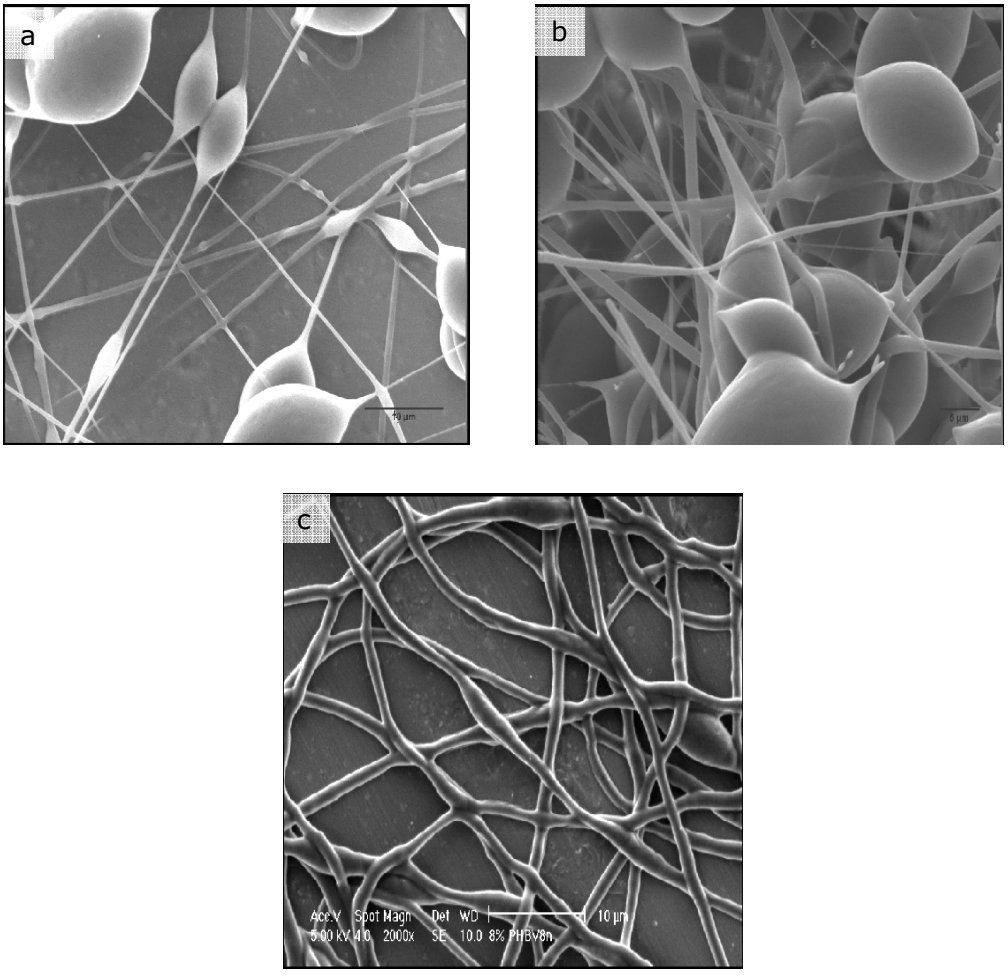

Figure 16. Effect of potential on fiber diameter and bead shape. Potential was (a) 20 kV, (b) 30 kV, and (c) 50 kV. PHBV was 8 % (w/v) in chloroform. Original magnification: x2000.

Bead shape changed from spherical to spindle shape or beads disappeared completely upon further potential increase.

Higher potentials are known to result in higher electrostatic forces and higher drawing stresses on the jet, leading to fibers with smaller diameters [89, 90, 116]. It is stated that low potentials might be barely sufficient to exceed the limit for Taylor cone formation and jet formation, and fibers formed have larger diameters due to the large decrease in surface charges and field strength with distance. Katti and his co-workers (2004), on the other hand, have also shown that an increase above a certain potential does not lead to a significant change on fiber diameter [90]. Since, in the current study, the fiber diameter change with potential was not that significant, the system appears to have already reached this "potential insensitive" region.

3.1.2.3. Influence of Distance (Length of the Trajectory)

In the current study, it was observed that fibers could be obtained when chloroform was the solvent even when the trajectory was short (i.e. 20 cm) because its evaporation rate is high. At low polymer concentrations (i.e. 5%), however, fibers fused and a porous film instead of a fibrous structure was obtained (*Fig. 17*).

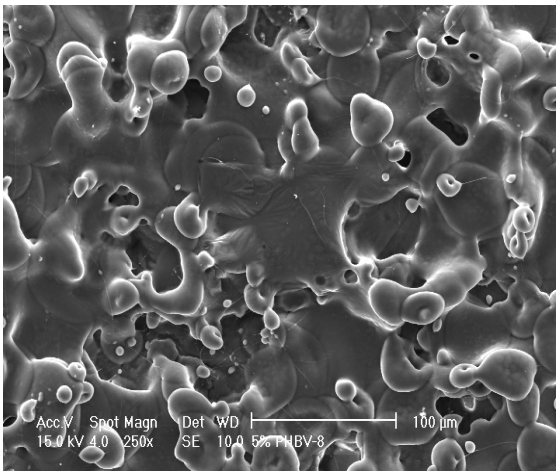

Figure 17. Film formation at very low PHBV concentrations (5% (w/v)) in chloroform (original magnification: x 250).

When the distance was increased to 35 cm, formation of wet films was prevented, bead formation was reduced but no significant influence on fiber diameter was observed. This is in contrast to Baker *et al (2006)* who found an inverse relationship between the distance and the fiber diameter and could possibly be explained by the other differences in between the two systems, such as polymer type, the concentration and the potential [118].

As a result, the optimum trajectory range was chosen to be 20-35 cm range in the rest of this study.

3.1.2.4. Influence of Solvent on Fiber Morphology

Solvent choice is very important in obtaining good fibrous scaffolds. In the current study, initially chloroform was used because it is a good solvent for PHBV. However, it was observed that the resultant mesh had non-porous beads in their structure, a property not desired. Moreover, the dimension and form of the fibers were not uniform and the fibers were not straight. Addition of BTEAC salt (2 %) to $CHCl_3$ *(Fig. 18a)* improved the results compared to that in pure $CHCl_3$ *(Fig. 15c)*; less beads and more uniform nanofibers were obtained. It, however, also led to fiber fusion.

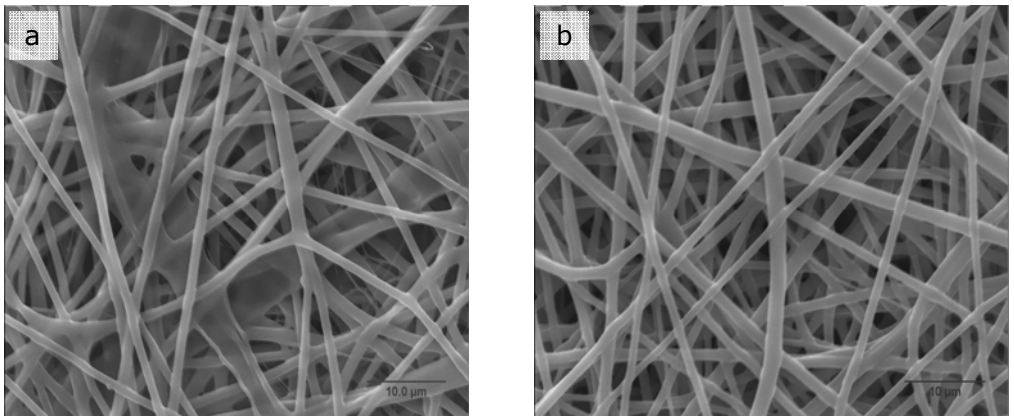

Figure 18. Influence of solvent on PHBV (15% w/v) fiber properties. (a) BTEAC salt added to chloroform, and (b) DMF added to chloroform ($CHCl_3$:DMF (96:4)) (original magnification: x2000).

As expected from the results in section *3.1.2.1*, fiber fusion decreased when the polymer concentration was increased (from 7 to 15 %, w/v) (data not shown). Lower number of defects (nicks) in the fibers were observed when the salt was present (compare *Fig. 15c,* indicated by the arrows, and *Fig. 18a*). Addition of 2% BTEAC salt in the $CHCl_3$ solution of PHBV (15% w/v) decreased the PHBV fiber diameter from 2200 ± 716 nm to 1254 ± 355 nm *(Table 4)*.

These results are consistent with those reported earlier by Lee *et al.* (2005) who observed a similar effect upon using NaCl salt on poly(2-acryloamido-2-methyl-1-propane sulfonic acid) fibers [119].

Another processing parameter modification that was investigated to improve the fiber quality was to add another solvent, DMF, with a higher dielectric constant (36.7 $C^2m^{-2}N^{-1}$ at 25ºC) to the existing solvent. Higher dielectric constant would increase the conductivity of the polymer solution leading to higher net charges in the solution, and the higher attractive forces created between the metal collector and the syringe tip would lead to more straight and uniform fibers. As predicted, fibers with better and uniform morphology, and no fusion and beads were obtained *(Fig. 18b)*. The thickness of the fibers obtained using polymer concentrations of 7, 10 and 15 % (w/v) were 723 ± 260 nm, 862 ± 296 nm, and 1166 ± 248 nm, respectively, showing that the fibers produced in the higher dielectric constant solvent mixture were thinner in comparison to those obtained with pure $CHCl_3$ as solvent *(Table 4)*.

As a result, all the samples planned for use in cell culture studies were prepared using PHBV dissolved in chloroform:DMF (96:4) mixture without any salt addition.

3.1.2.5. Influence of Polymer Type

An advantage of using the electrospinning process to produce nanofibrous scaffolds is that a variety of polymer compositions and blends can be utilized with ease. In this way, the limitations of individual homo- or copolymers can

be overcome. In the present study, PHBV was used alone or as blends with PLLA, P(L,DL)LA (70:30), PLGA (75:25), and PLGA (50:50) in a 1:1 (w/w) ratio in order to study the influence of polymer type on electrospun fiber properties. All the blends were dissolved in chloroform:DMF (96:4). It was not possible to compare all the polymer blends at the same concentration because while the first two blends could not be spun when the concentration was high (7.5%), the other two could not be spun when it was low (5%). Thus, the concentrations tested for the blends were: 5% (w/v) for PLLA and P(L,DL)LA (70:30), and 15 % (w/v) for PLGA (75:25) and PLGA (50:50).

Blends exhibited different behaviors under the same process conditions (distance: 35 cm, potential: 30 kV, needle diameter: 22 gauge, and needle length: 10 mm). Under these conditions, while the blend with PLLA produced thin (diameter: 377 ± 97 nm) and beaded fibers, the blend with P(L,DL)LA (70:30) resulted in much thicker (diameter: 1509 ± 283 nm) and bead-free fibers *(Table 4)*. Under the same conditions 5 % (w/v) pure PHBV behaved more like the blend with PLLA and led to thin fibers (284 ± 133 nm) with a large number of beads. 15% (w/v) PHBV-PLGA (75:25) blend resulted in fibers with large, spherical beads and an average fiber diameter of 978 ± 377 nm whereas PHBV-PLGA (50:50) fibers had spindle-shaped beads and much higher fiber thickness (1176 ± 289 nm) *(Fig. 19)*. Under the same conditions, unblended 15 % (w/v) PHBV led to much thicker fibers (2200 ± 716 nm) and no beads. It appears from these results that concentration is at least as influential on fiber properties (thickness, bead formation) as the polymer type.

It is not a simple task to explain why a decrease of the lactic acid component of PLGA would lead to such significant changes on fiber characteristics. Similarly, highly crystalline PLLA in the blend significantly decreases the diameter and increases bead formation. These studies must be followed up with a larger number of PLGAs with different copolymer compositions in order to be able to bring forth a molecular explanation.
In the end, PHBV-PLLA, PHBV-P(L,DL)LA (70:30) and PHBV-PLGA (50:50) blends were considered to be more suitable for tissue engineering studies and PHBV-PLGA (75:25) blend was left out.

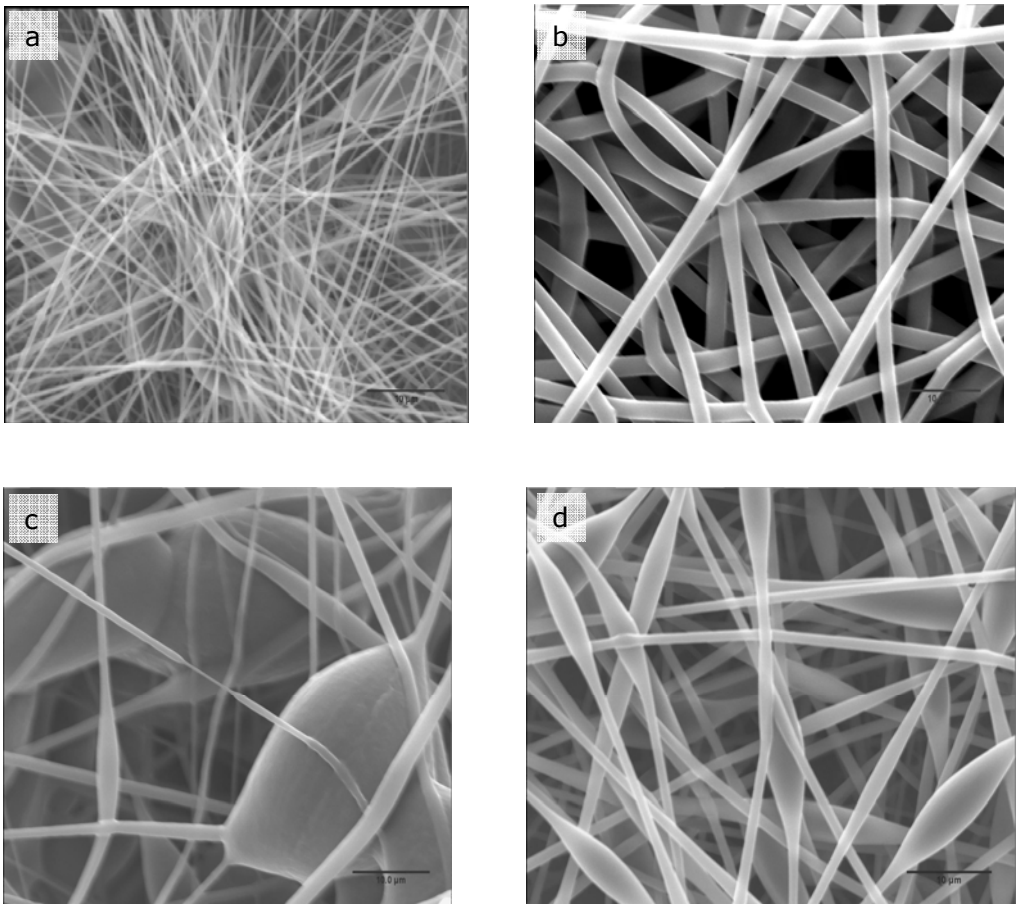

Figure 19. Influence of polymer type on fiber shape and thickness. (a) PHBV-PLLA, (b) PHBV-P(L,DL)LA (70:30), (c) PHBV-PLGA (75:25), and (d) PHBV-PLGA (50:50). Polymer concentrations in a and b are 5% (w/v) whereas in c and d they are 15% (w/v). Solvent: $CHCl_3$:DMF (96:4); Distance: 35 cm; Needle length: 10 mm, and Potential: 30 kV. Original magnification: x2000.

3.1.2.6. Alignment of pure PHBV and PHBV blends

In order to develop tissue engineering scaffolds with fibers having a predetermined orientation the polymers were dissolved in $CHCl_3$:DMF (96:4) and electrospun onto a rotating collector (2000 rpm). The fibers were wound around the collector as they were produced and it was possible to obtain aligned nano/microfibers with different thicknesses (*Fig. 20*).

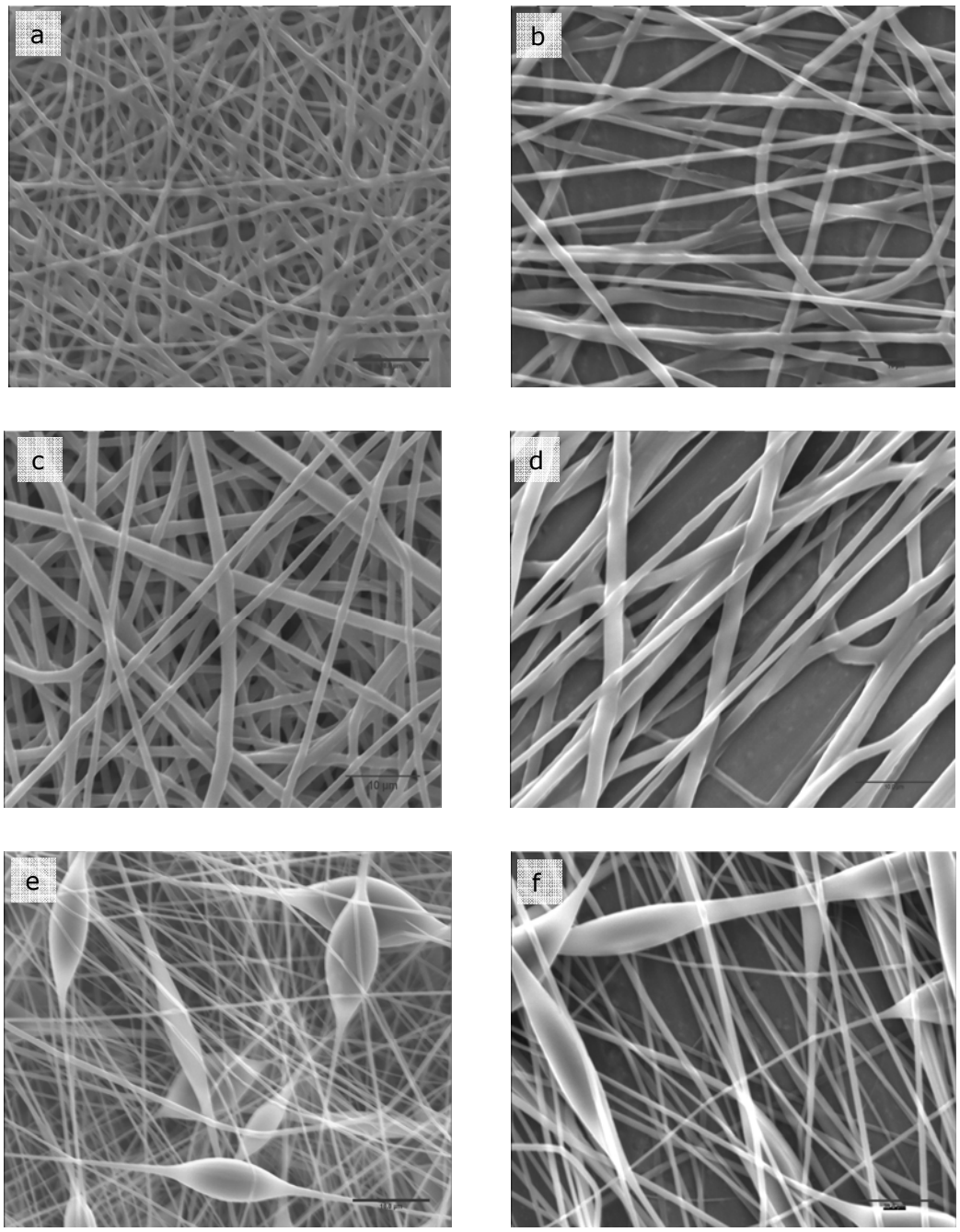

Figure 20. Influence of fiber collection method (and orientation) on fiber properties. Pure PHBV (10 and 15% (w/v)) and its blends in $CHCl_3$:DMF (96:4) were electrospun as: (a, c, e, g and i) unoriented fibers (Distance: 30 cm; Needle length: 10 mm and Voltage: 30 kV), and (b, d, f, h and j) aligned fibers (Distance: 25 cm; Needle length: 10 mm and Voltage: 20 kV). (a and b) 10% (w/v) PHBV; (c and d) 15 % (w/v) PHBV; (e and f) 5 % (w/v) PHBV-PLLA; (g and h) 5 % (w/v) PHBV-P(L,DL)LA and (I and j) 15 % (w/v) PHBV-PLGA (50:50). Original magnification: x2000.

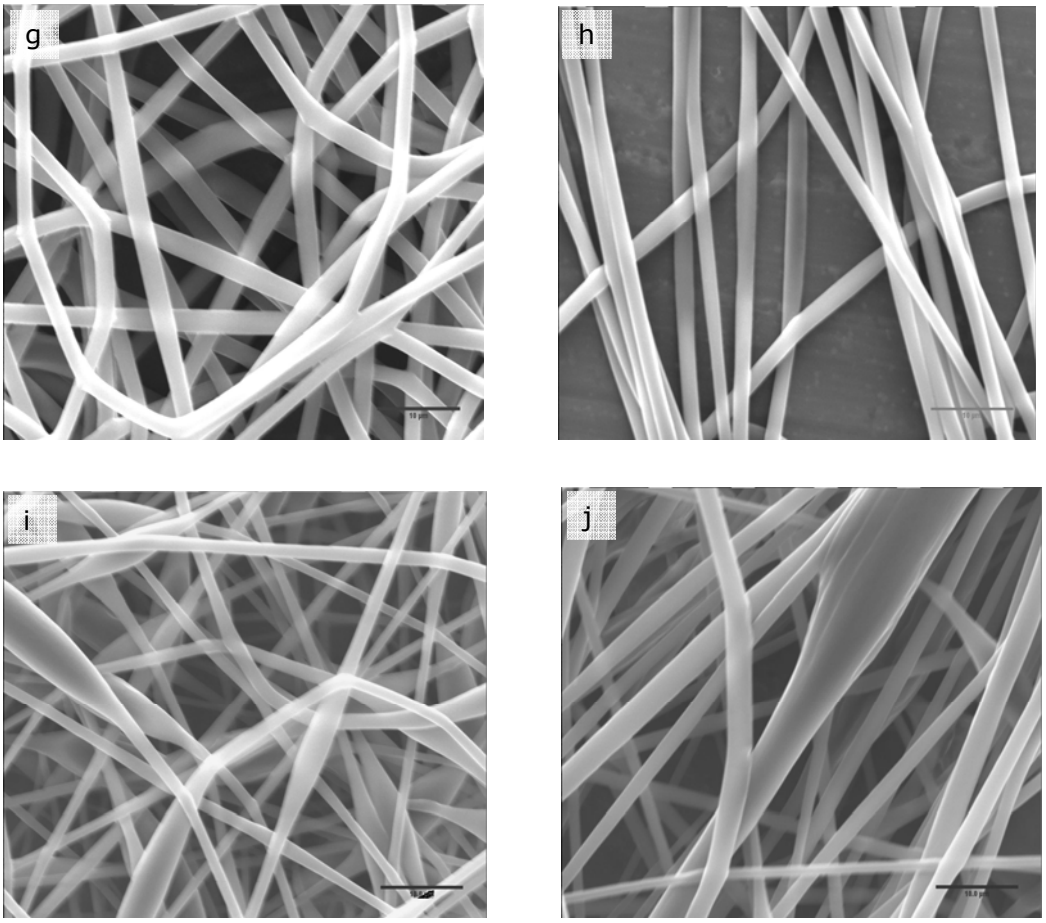

Figure 20. (continued)

Fibers obtained with a rotating collector were expected to be thinner than with the static collector produced under the same conditions because rotation was expected to create higher attractive forces that would lead to thinning of the fibers. The strain of the fibers due to the rotation would also contribute to this thinking. However, this was not observed. Unaligned and aligned PHBV (15 %) fibers had diameters of 1166 ± 248 nm and 1309 ± 513 nm, respectively. Fiber thicknesses of aligned PHBV-PLLA, PHBV-P(L,DL)LA (70:30) and PHBV-PLGA (50:50) blends were also found to be significantly increased (450 ± 218 nm vs. 377 ± 97 nm, 1972 ± 266 nm vs. 1509 ± 283 nm, 1632 ± 530 nm vs. 1176 ± 289 nm, respectively) *(Fig. 20)*.

3.2. Surface porosity of electrospun nano/microfibers

The upper surface porosity of the nano/microfibers was assessed from their SEM micrographs (JEOL Ltd., T100, Japan) microscope using NIH Scion Image program. The results are presented in *Table 5*.

Table 5. Surface porosity of various polymeric nanoscaffolds obtained by electrospinning process.

Polymer type and Concentration	Surface porosity (%)
PHBV (10% (w/v))	38.0 ± 3.8
PHBV (15% (w/v))	40.1 ± 8.5
PHBV-PLLA (5% (w/v))	53.8 ± 4.2
PHBV-P(L,DL)LA (5% (w/v))	50.0 ± 4.2
PHBV-PLGA (50:50) (15% (w/v))	30.8 ± 2.7

The results reveal that the highest surface porosity is obtained with the PHBV-PLLA blend closely followed by PHBV-P(L,DL)LA, PHBV (15% (w/v)), PHBV (10% (w/v)) and finally PHBV-PLGA. As mentioned above, these numbers are based on using high contrast SEMs, and therefore, the values presented represent the data from the top 7-10 layers of fibers, and are, therefore, much lower than the actual values (when several fiber layers are observed from the top fibers of various layers appear as if they are at the same level and thus the porosity turns out to be much smaller than reality). It is expected that porosity of nanofibrous scaffolds should influence the cell behavior and that higher porosity should lead to higher cell adhesion, proliferation and differentiation. This will be discussed further in the following sections.

3.3. *In vitro* studies

Many researchers have reported that nanofibers can support the attachment of a variety of cells, maintain their phenotype and guide their growth [25, 26, 35, 37, 106, 116]. Li and coworkers (2002) reported that their nonwoven nanofibers produced by electrospinning process were nano-sized and suitable for tissue engineering since their high porosity, the broad range

of pore diameters and mechanical properties mimic the architecture of the natural ECM [35].

There are some criteria that an electrospun scaffold should meet before being used in 3D tissue culture experiments. It should be strong enough to handle so that it does not fragment during the experiments. Its surface topography and chemistry should be suitable since it has been shown that they play a crucial role in cell adhesion, proliferation, and eventually, in new tissue formation [116, 118]. The polymer utilized in this study was PHBV and some of its blends with lactide-based polymers. PHBV itself is highly hydrophobic, thus, some surface modification was done in order to increase cell performance on the scaffolds. The following *in vitro* studies were performed to observe the suitability of these electrospun scaffolds for bone tissue engineering.

3.3.1. SaOs-2 cell proliferation on electrospun fibers

SaOs-2 numbers were measured by MTS assay, which helps calculate the cell density on the scaffolds. All the scaffolds were seeded with these and the proliferation rates were calculated on Days 1, 7 and 14 after seeding. The initial cell density for each carrier was $5x10^4$ cells/cm2. The same cell density was achieved on tissue culture polystyrene flasks (TCPS) in order to be able to compare the proliferation rates. The cell numbers on TCPS on the Days 1, 7 and 14 after seeding were found to be $5.2x10^4$, $2.1x10^5$ and $1.4x10^5$ cells/cm^2 (*Fig. 21*). When the cell density is too high they undergo apoptosis leading to cell number decrease but their number increases again. This might be the reason why the cell number on Day 14 was lower than that on Day 7.

The cell numbers on oxygen plasma treated (5 min, 50 W) 10% PHBV carriers on Days 1, 7 and 14 were $2.0x10^4$, $7.1x10^4$ and $1.5x10^5$ cells/cm^2 whereas the untreated samples were found to have $1.2x10^4$, $3.4x10^4$ and $1.0x10^5$ cells/cm^2. The results show that there are a higher number of cells (almost double) when the surface is treated with oxygen plasma. The change, however, is not very significant demonstrating that a higher oxygen

plasma treatment for surface modification might be necessary in order to increase the cell number further.

When a carrier with the same polymer type but higher polymer concentration was used, the cell numbers on PHBV regardless of the treatment were very similar and much lower than the 10% PHBV case (data not shown). As shown in Table 4, as the polymer concentration is increased the fiber thickness increased and bead formation decreased. Thus, it can be concluded that cells prefer mats with lower diameters since their number was found to be higher in cell carriers with lower diameters.

Similar behavior was observed with PHBV-PLLA, with the PHBV-P(L,DL)LA, and with PHBV-PLGA (50:50) blends, too. The lowest cell numbers were observed with the PHBV-P(L,DL)LA blend. These results are consistent with those obtained by Moroni and his coworkers, who state that scaffolds with smaller diameter fibers result in higher cell attachment and proliferation due to the higher radius of curvatures offered by small diameters [101]. On the other hand, Badami et al (2006) have investigated the influence of fiber diameter on spreading, proliferation and differentiation of osteoblasts on PLLA substrates [24]. They also concluded that surface topography influences on cell behavior, however, their results showed an increase of cell density with increase in fiber diameter, which is in contrast with the results of this study.

In conclusion, cell proliferation studies revealed that regardless of the nanofiber type TCPS allows the cells reach confluency much faster, partially due to its surface chemistry but also due to its being in a film form while the others are fibrous mats. Among the fibers, PHBV from the more dilute solution (10%) and PHBV-PLLA blend were the most preferred scaffolds.

3.3.1.1. Effect of polymer type on SaOs-2 proliferation rate

Related to choosing the best carrier for engineering new bone tissues, the following Figure 21 shows this classification. It is obvious that in the case of oxygen plasma treated blends, PHBV-PLLA exhibited a similar behavior to TCPS, thus, maintaining its most favored surface/material status. This is followed by PHBV10, PHBV-PLGA (50:50), PHBV15 and finally PHBV-P(L,DL)LA blend.

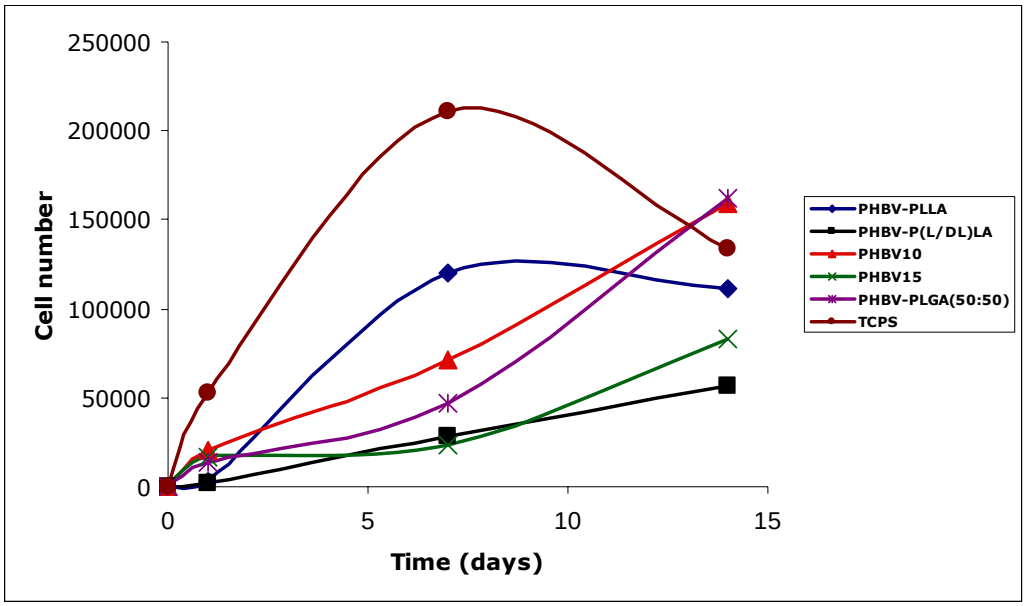

Figure 21. Proliferation of SaOs-2 cells on oxygen plasma treated blends.

If the blends are not oxygen plasma treated, the preference is slightly different. Again PHBV-PLLA appears to be the best, which is then followed by PHBV-PLGA (50:50), PHBV10, PHBV15 and finally PHBV-P(L,DL)LA blend (*Fig. 22*).

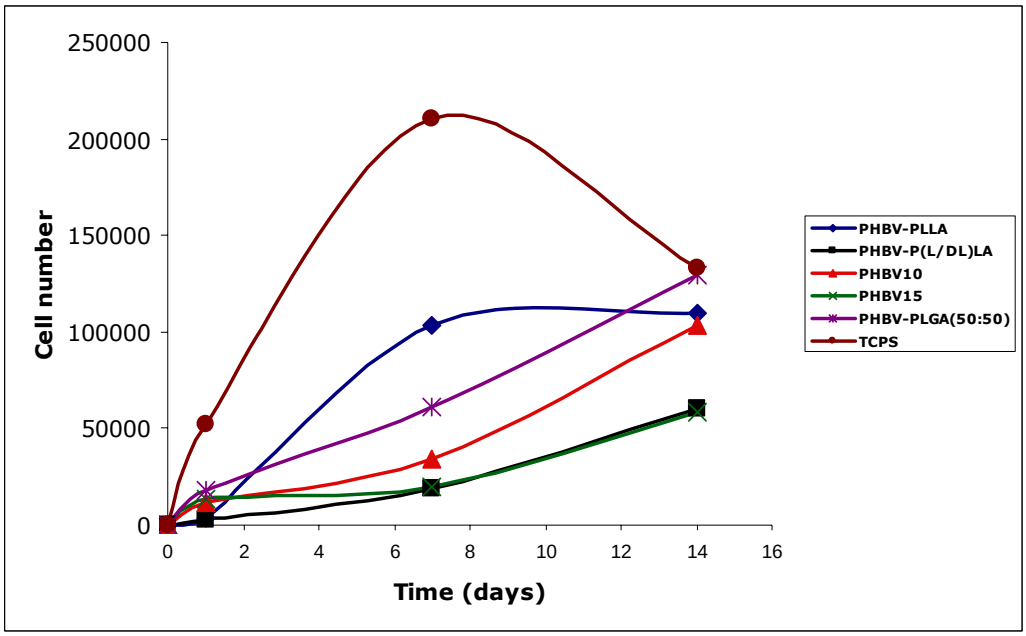

Figure 22. Proliferation of SaOs-2 cells on different untreated blends.

As presented in *Table 4* and section 3.1.2.5 the diameter of scaffolds varied with the polymer type used. The corresponding fiber thicknesses for PHBV-PLLA, PHBV10, PHBV-PLGA (50:50), PHBV15 and PHBV-P(L,DL)LA were calculated to be 377 ± 97 nm, 862 ± 296 nm, 978 ± 377 nm, 1166 ± 248 nm and 1509 ± 283 nm. It appears, therefore, that as the fiber diameter increases the cell number on the oxygen plasma treated cell carriers decreases. In other words, the thinner the fibers, the higher the proliferation rate of cells on these scaffolds. In the case of pristine samples, the order of preference for PHBV10 and PHBV-PLGA are changed, which might be as a result of some experimental errors while seeding or since the fiber diameters for these two scaffolds are close to each other, the effect of fiber thickness on SaOs-2 proliferation rate has not been that significant.

Figure 23 reveals very clearly the effect of diameter of fibers obtained from the same polymer, but at different polymer concentrations (10 and 15 % (w/v)), on proliferation rate of cells. This time again the higher is the diameter (PHBV15) the lower is the cell number adhering on the scaffold.

The difference is even more distinct in the case of oxygen plasma treated carriers.

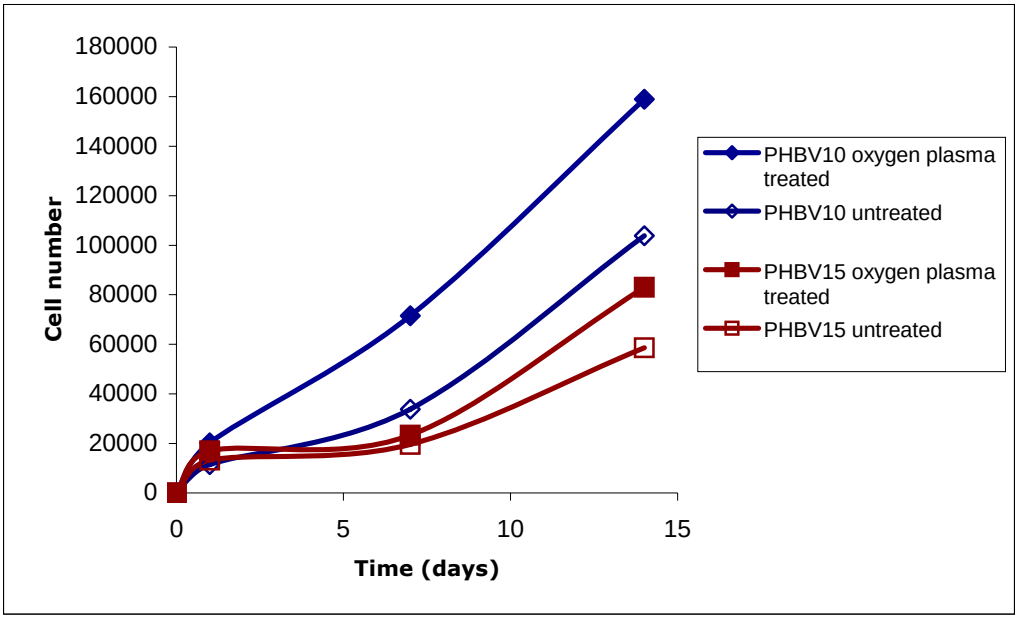

Figure 23. Proliferation of SaOs-2 cells on scaffolds obtained with oxygen plasma treated and untreated fibers obtained with 10 and 15 % (w/v) PHBV solutions.

Influence of argon plasma treatment on cell attachment was investigated by Badami *et al.* (2006), who observed a two-fold increase of cell attachment in case of plasma-treated, electrospun polystyrene scaffolds compared to the untreated ones [24]. This was explained as a result of enhanced wettability caused by incorporation of oxygen containing groups such as hydroxyl, carboxyl and carbonyl. It is clear that these results are consistent with the results obtained in this study even though in the present study a more extensive oxygen plasma treatment might have resulted in a better cell-to-material interaction.

3.3.2. Microscopy studies

3.3.2.1. Cell morphology

All the scaffolds were examined with SEM on Days 7 and 14 of seeding (*Fig. 24*). Scaffolds obtained from 10% PHBV8 solutions showed an even distribution of cells on the surface and a good cell-to-cell and cell-to-scaffold interaction. As expected, the scaffold surface was much more populated on Day 14 for both the untreated and oxygen plasma treated carriers.

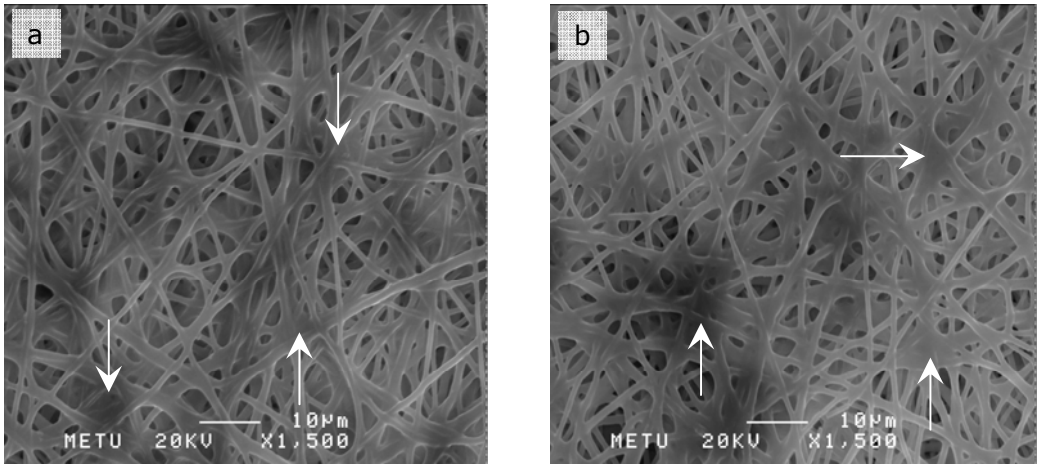

Figure 24. SEM micrographs of SaOs-2 cells on (a) untreated, and (b) oxygen plasma treated PHBV10 scaffolds 7 days after incubation (original magnification: x1500). Arrows indicate cells.

It was observed that cells accumulated more on the surface than in the body of the scaffolds. A reason for this can be the fact that surface porosity of this scaffold was among the lowest of the tested ones.

The in vitro response of the scaffold obtained from pure PHBV solution with a higher concentration (15%), and thus with higher fiber thickness, was examined (*Fig. 25*).

A lower cell number was expected to adhere on this type of cell carrier, since cells have been shown to prefer fibrous environments with diameters

close to cell size [26, 71] and the MTS results of this study supported this expectation. However, SEM micrographs exhibited a good distribution of cells on the surface and even penetration of the cells inside the scaffolds was observed.

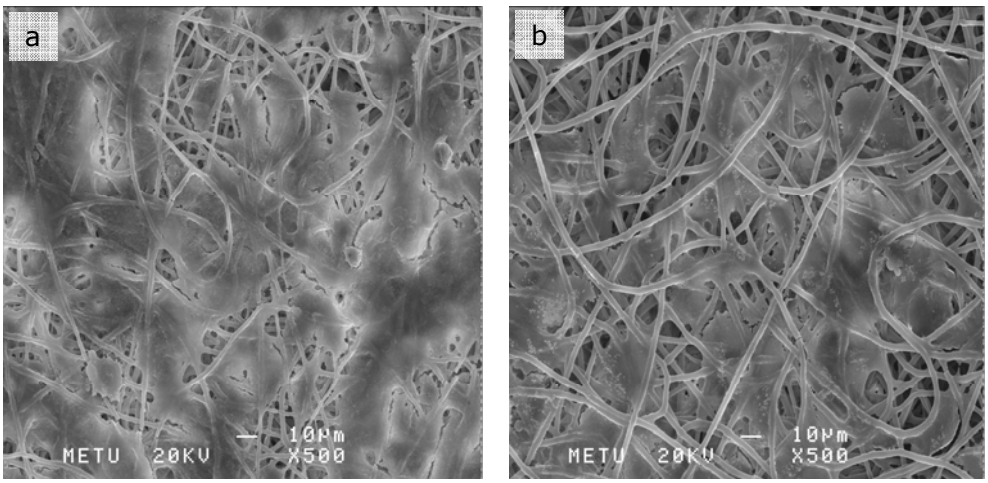

Figure 25. SEM micrographs of SaOs-2 cells on (a) untreated, and (b) oxygen plasma treated PHBV15 scaffold 7 days after incubation (original magnification: x500).

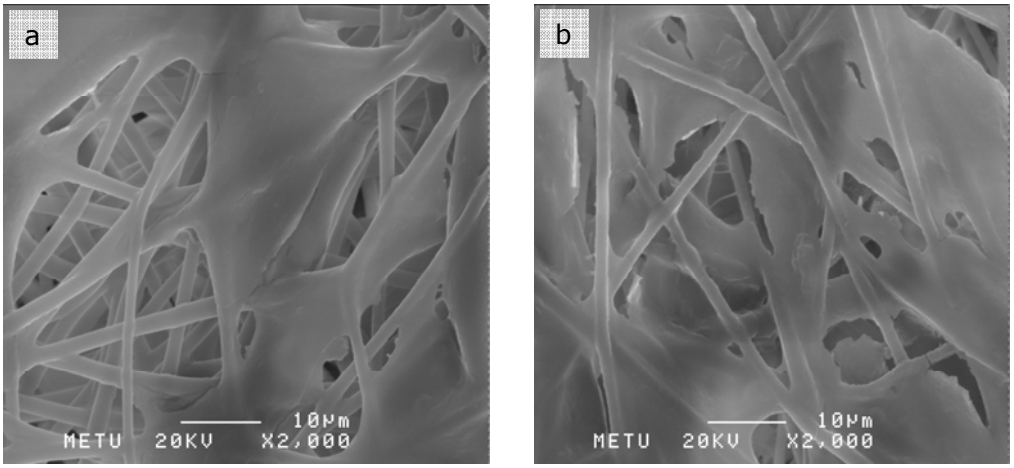

Figure 26. SEM micrographs of SaOs-2 cells on (a) untreated, and (b) oxygen plasma treated PHBV-P(L,DL)LA scaffold 14 days after incubation (original magnification: x2000).

Even though the MTS test with the PHBV-P(L,DL)LA blend showed the worst cell adhesion and proliferation performance, SEM micrographs showed a good distribution of cells (*Fig. 26*). Cells agglomerated at certain parts of the carrier; their distribution, however, was homogeneous, and cell-to-cell and cell-scaffold interaction appeared to be satisfactory.

Again it is observed that cells were mainly localized on the surface of the scaffold and it did not appear to be very crucial whether the surface was modified or not because cell behavior seems to be approximately the same. Maybe a higher level (higher duration and power) of oxygen plasma treatment would improve the results.

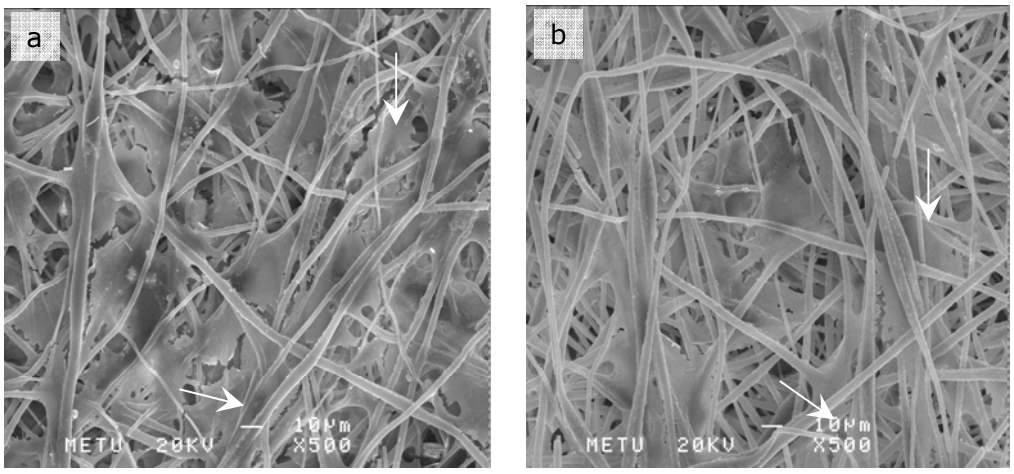

Figure 27. SEM micrographs of SaOs-2 cells on (a) untreated, and (b) oxygen plasma treated PHBV-PLGA scaffold 7 days after incubation. Arrows indicate cell-to-cell connection (original magnification: x500).

Both untreated and plasma treated PHBV-PLGA scaffolds showed similar performance (*Fig. 27*). In this case the scaffolds contained beads, and the cells used these beads as bridges to connect to their neighboring cells. Rather than being on the surface of the carrier, cells were present more on the inside of the scaffold. Compared to the above mentioned scaffolds, the cells in this scaffold were more distributed and were spread over the whole scaffold, even though not very homogeneously.

MTS results revealed that PHBV-PLLA blend would be the most suitable scaffold because cell proliferation rates on this carrier were the highest among the oxygen plasma treated and untreated samples. In the SEM, the cells are seen to spread uniformly over the whole scaffold and a significant level of cell penetration was observed (*Fig. 28*).

PHBV-PLLA carrier had the lowest fiber diameter and contained spindle-shaped beads. Despite the beads, the cells were well distributed and as in the case of PHBV-PLGA blend, the cells were spread around and over the beads. The highest surface porosity was observed with this scaffold (*Table 5*), and this might have been a reason for the good cell penetration into fiber substrates observed in this carrier.

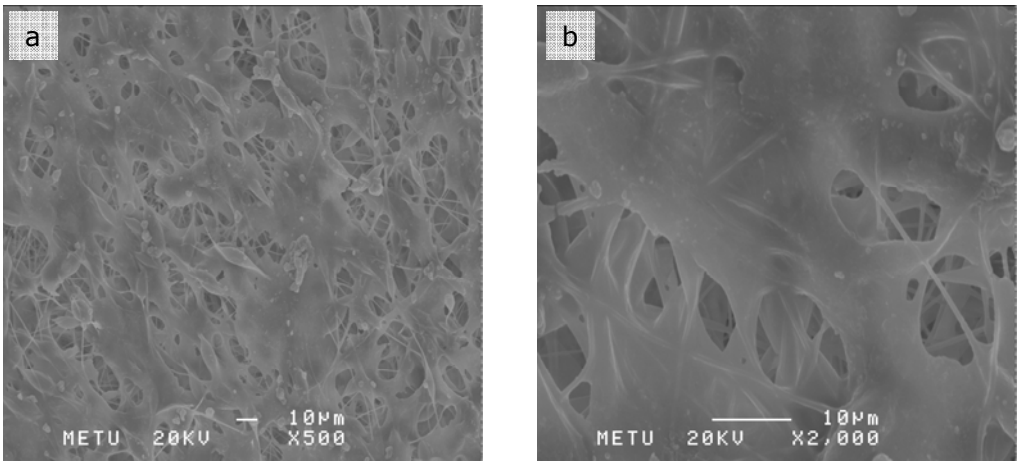

Figure 28. SEM micrographs of SaOs-2 cells on (a) and (b) untreated, and (c) and (d) oxygen plasma treated PHBV-PLLA scaffold 7 days after incubation (original magnification: (a) and (c): x500; (b) and (d): x2000).

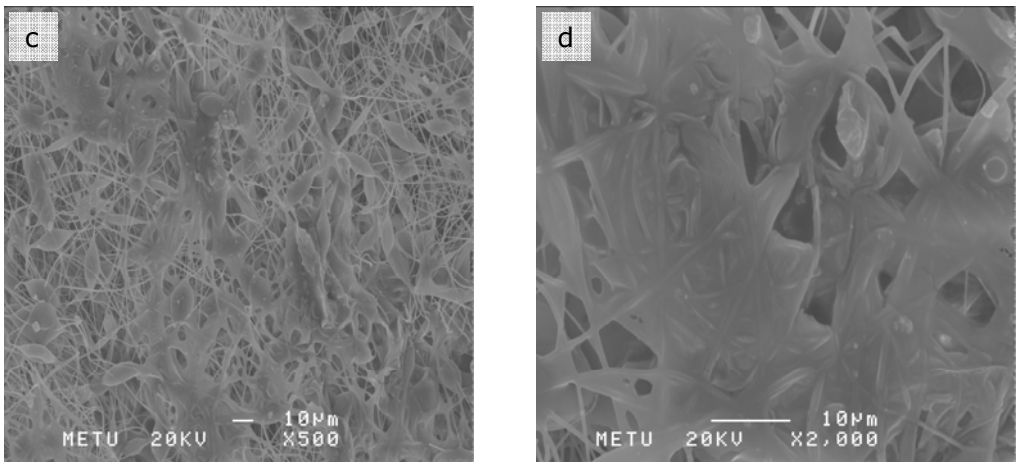

Figure 28. (continued)

3.3.2.2. Cell staining (FITC-labeled phalloidin and DAPI staining)

FITC-labeled phalloidin staining was performed in order to observe the orientation and spreading of SaOs-2 cytoskeletal actin filaments. In addition DAPI staining was used to observe the nucleus of the cells. Therefore, double staining was performed in order to observe both the cytoskeleton (and shape of SaOs-2 cells), their interaction with the fibrous scaffolds and their nuclei. In some micrographs cells were observed to aggregate at certain regions of the scaffolds, whereas some other regions were completely uninhabited. This might be due to the fact that scaffold porosity obtained by electrospinning is not the same everywhere since the resultant fibers are collected randomly on the target and are collected more where charge attraction is higher. Oxygen plasma seems to have improved this situation and led to better spreading and cell-to-cell contact (compare *Fig. 29a with 29c*).

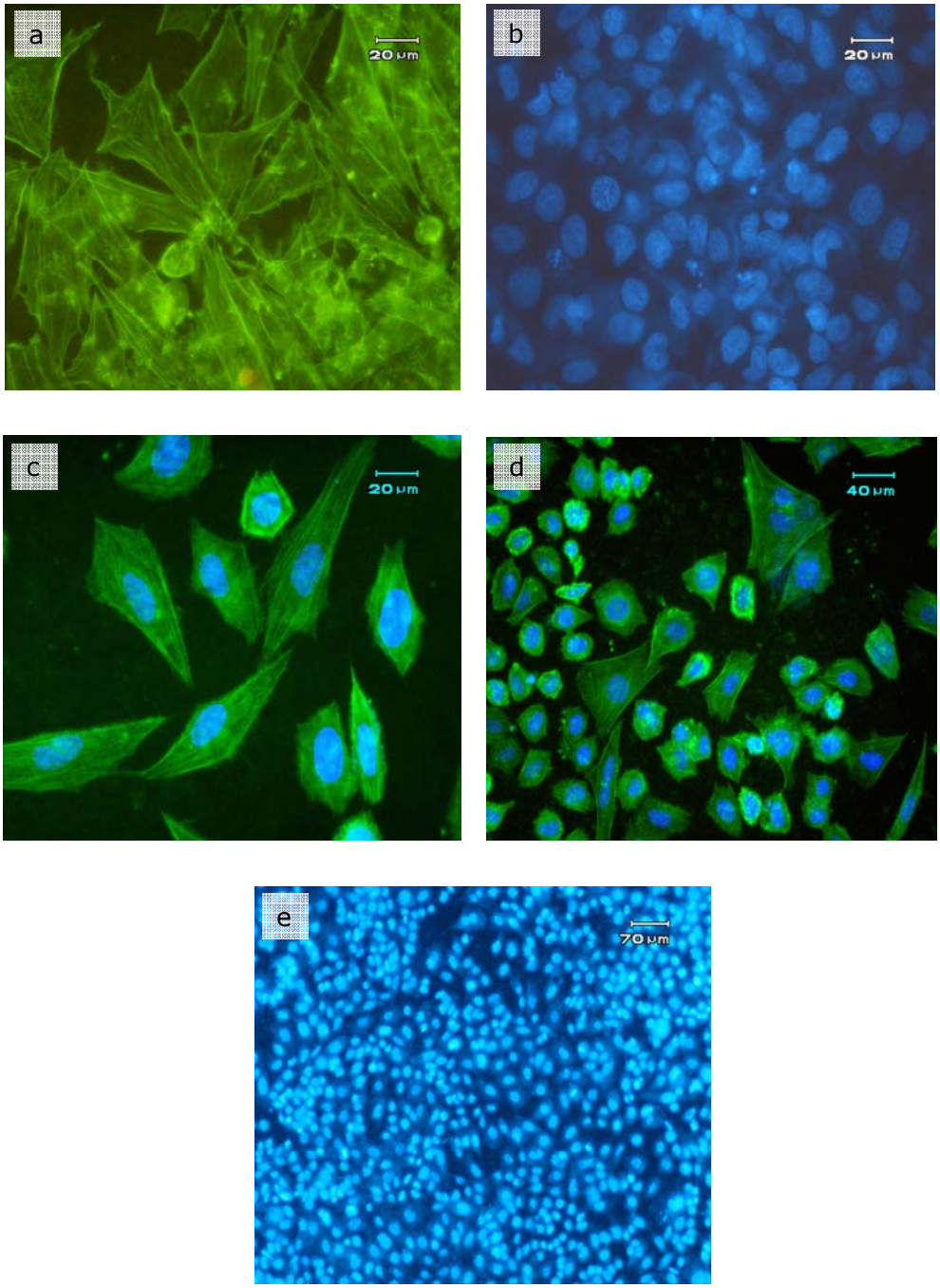

Figure 29. Fluorescence micrographs of: (a, c) FITC-labeled phalloidin and (b, d, e) DAPI stained SaOs-2 cells on (a and b) oxygen plasma treated and (c, d and e) untreated PHBV10 scaffolds. 7 days after incubation.

When the cell behavior on these five different carriers are compared it can be stated that more cells were present on PHBV10 (*Fig. 29e*) and PHBV-PLLA blend (*Fig. 33*), which is consistent with the quantitative results obtained by SaOs-2 proliferation profiles (MTS tests). In none of the cases a very distinct difference between the oxygen plasma treated and untreated blends was observed.

Fig. 30 presents the structure of SaOs-2 cells on PHBV15 carriers. Compared to cell behavior on PHBV10, it was observed that cells in this case are not spread as well.

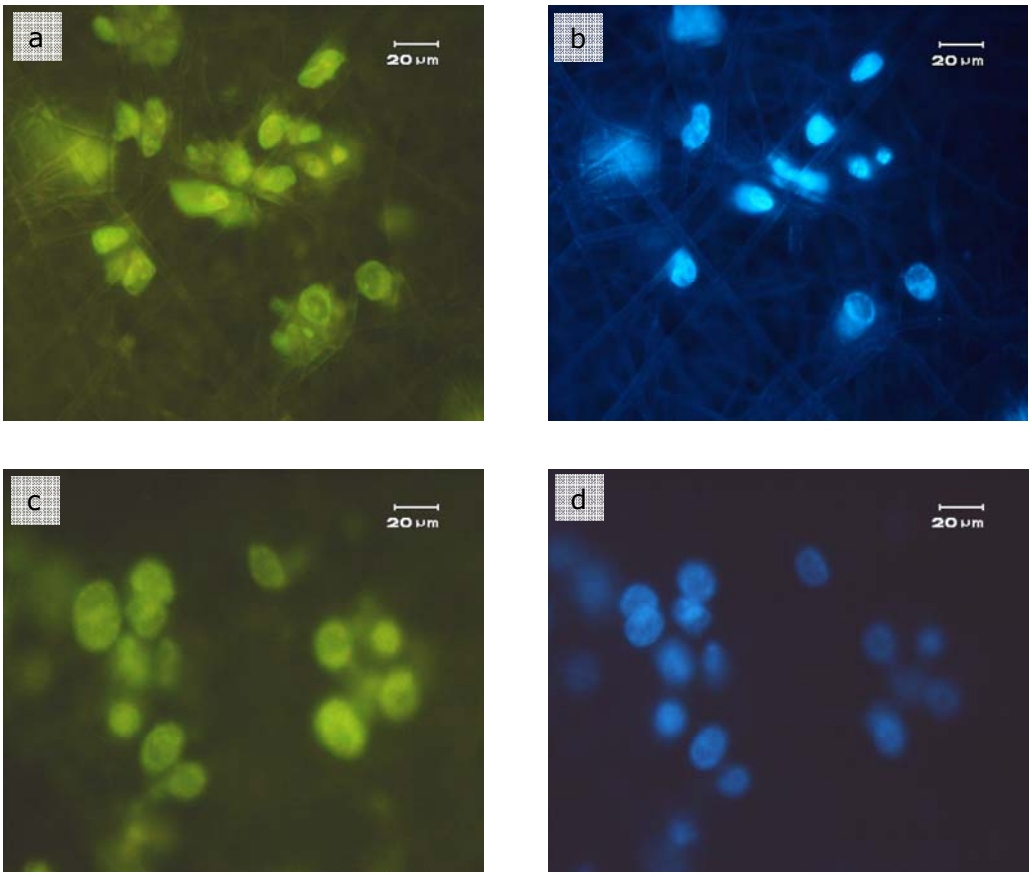

Figure 30. Fluorescence micrographs of FITC-labeled phalloidin (a, c) and DAPI stained (b, d) SaOs-2 cells on (a, b) oxygen plasma treated and (c, d) untreated PHBV15 scaffolds 7 days after incubation.

The MTS data had revealed that the cell number in PHBV10 was higher than on PHBV15 and this low cell number was explained by increase in fiber diameter (*Fig. 30*). There was no distinct difference between the plasma treated and untreated carriers in relation to cell attachment.

The interaction between the fibers and cells could be more easily observed in the case of PHBV-P(L,DL)LA and PHBV-PLGA blends because these fibers were in the micro scale, and therefore, they could be observed with the magnification power of the fluorescence microscope (*Figs. 31 and 32*).

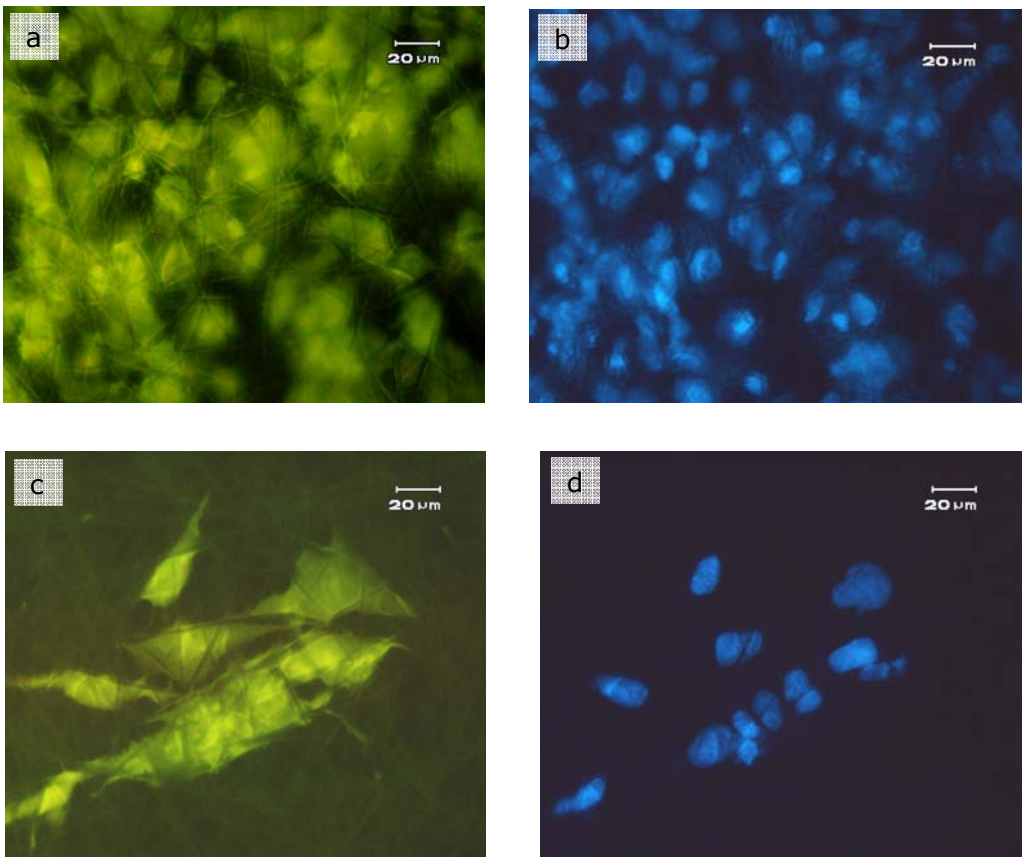

Figure 31. Fluorescence micrographs of (a, c) FITC-labeled phalloidin and (b, d) DAPI stained SaOs-2 cells on PHBV-P(L,DL)LA scaffolds 7 days after incubation. (a, b) were oxygen plasma treated, and (c, d) were untreated.

Cell confluency in PHBV-P (L, DL) LA blend (*Fig. 31*) was too low compared to all other cases. The high surface porosity of this blend was suitable for

appropriate distribution of cells over the scaffold but the scaffold material and the high fiber thickness created a poor environment for cell attachment. Plasma modification did not lead to a distinct difference ion terms of cell-material interaction.

With PHBV-PLGA (50:50) blend the cells were spread over and within the carrier, exhibiting extensive cell-matrix interaction. Even though quite large beads were present on this scaffold, cells showed a high cell proliferation rate. Both unmodified and surface modified carriers revealed similar behavior.

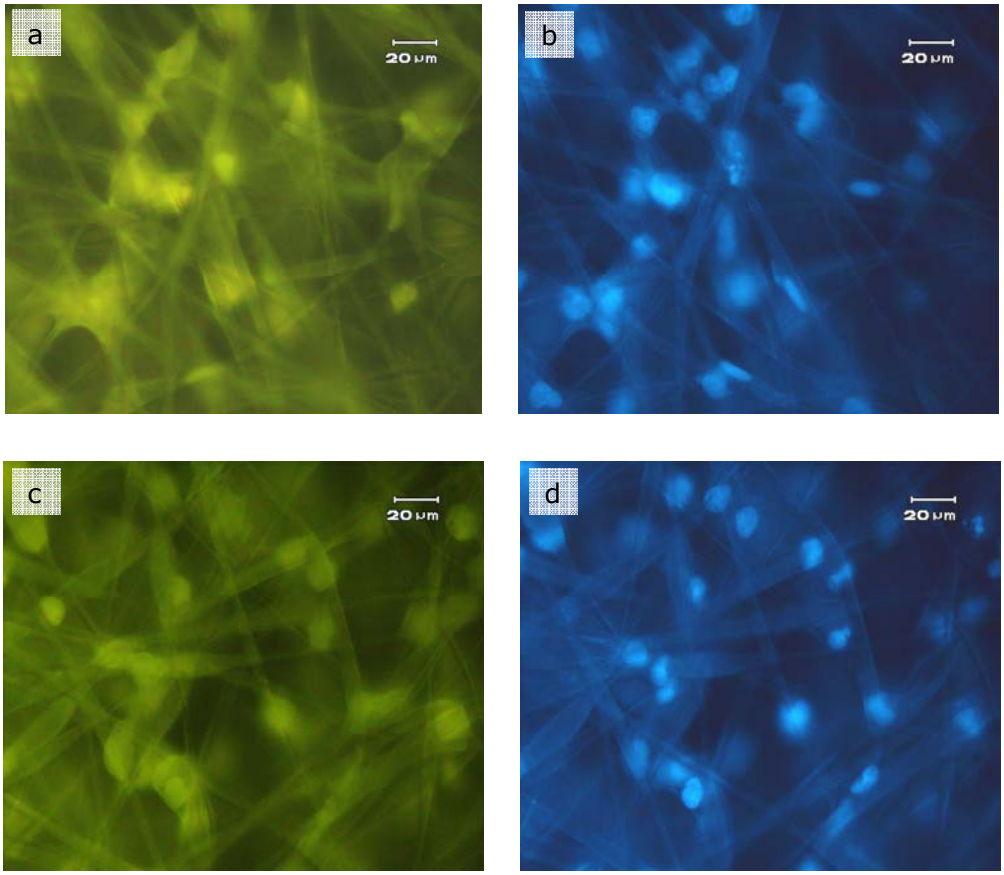

Figure 32. Fluorescence micrographs of (a, c) FITC-labeled phalloidin and (b, d) DAPI stained SaOs-2 cells on PHBV-PLGA (50:50) scaffolds 7 days after incubation. (a, b) oxygen plasma treated, and (c, d) untreated.

PHBV-PLLA was the best in the MTS tests (cell proliferation). *Fig. 33* shows that it is also the best in terms of cell shape and cytoskeleton orientation and distribution. Cells were well attached on the scaffold and furthermore they were higher in number compared to all the other blends. In this case too there was not a very large difference between the treated and untreated samples.

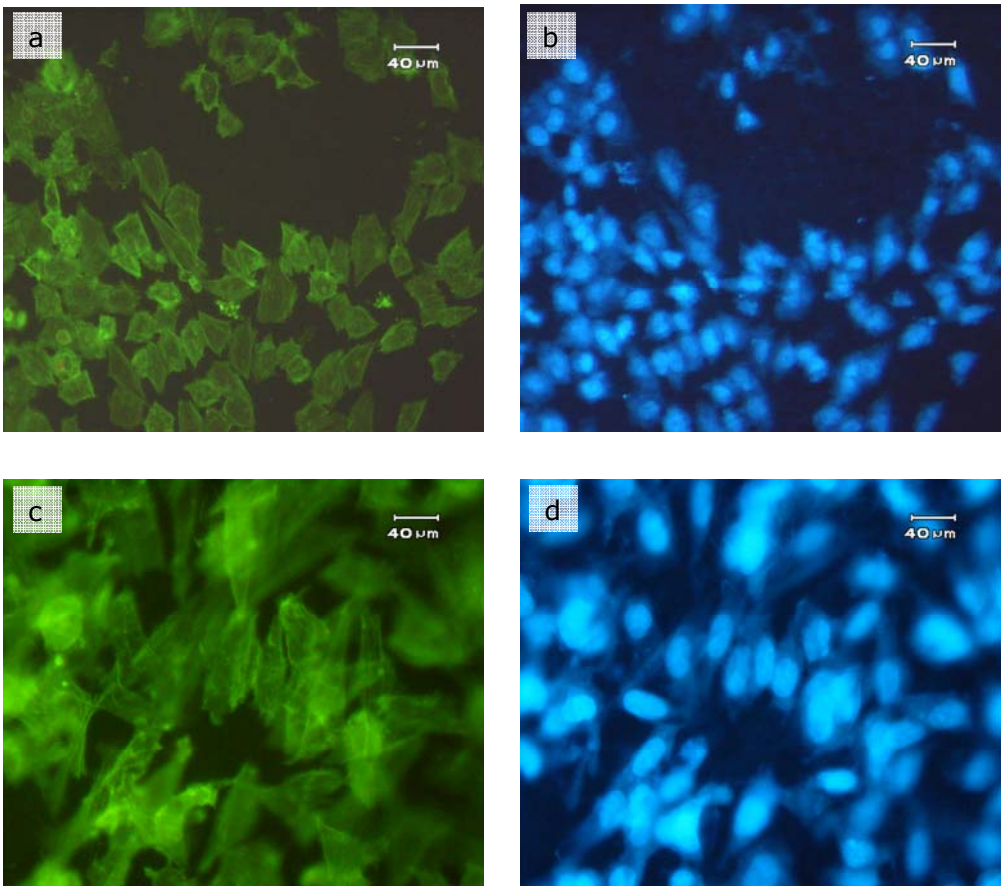

Figure 33. Fluorescence micrographs of (a, c) FITC-labelled phalloidin and (b, d) DAPI stained SaOs-2 cells on PHBV-PLLA scaffolds 7 days after incubation. (a, b) oxygen plasma treated, and (c, d) untreated.

3.3.2.3. Confocal Laser Scanning Microscopy (CLSM)

Apart from a highly biocompatible material surface, tissue engineering requires a three-dimensional structure that is appropriate for cell attachment, growth and migration. Confocal microscopy was used in this study to assess the distribution of cells within the fibrous structure of the scaffolds. SaOs-2 cells seeded on all types of scaffolds utilized in this study, were found to have appropriate interaction with their environment.

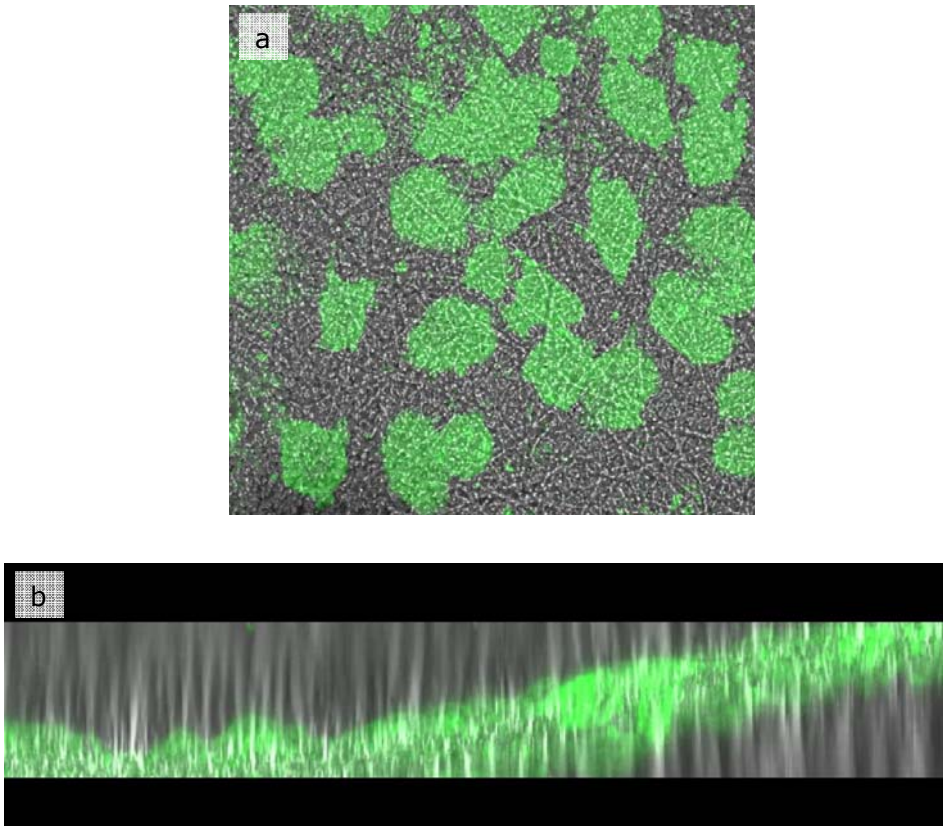

Figure 34. CLSM images of SaOs-2 seeded PHBV10 scaffolds 7 days after incubation. (a) top view distribution and penetration of the human osteosarcoma cells inside the scaffold showing the cell-matrix interaction (Magnification: x40), (b) distribution of osteosarcoma cells within the scaffold as viewed in cross section (Z-axis direction) (Magnification: x40). Staining is with Acridine orange.

As mentioned in the earlier sections, in addition to being attached on the surface of the scaffolds, cells penetrated the interior parts of the scaffolds, too. The most uniform distribution within the scaffold was seen in the case of PHBV-PLLA blend; however, the other scaffolds also exhibited a satisfactory distribution. Figure 34 is a good presentation of cell-matrix interaction and penetration of cells into the scaffolds. *Fig. 34b* shows clearly the distribution of cells throughout the scaffold indicating the suitability of these scaffolds for bone tissue engineering.

CHAPTER 4

CONCLUSION

Mimicking the structure and function of natural ECM is one of the most important requirements in tissue engineering. Upon implantation of the properly designed scaffold, carrying the desired type of cells, into the target tissue, effective repair can be realized. An ideal scaffold is one that possesses appropriate biodegradability, biocompatibility, mechanical properties to withstand the stresses that might occur in the newly formed tissue, and high porosity and permeability to allow entrance of the nutrients necessary for cell growth. PHBV was the main material utilized in this study due to its proven biocompatibility, biodegradability and versatility.

In this study, two fiber forming processes, wet spinning and electrospinning were used to create fibrous scaffolds with appropriate tissue engineering properties. After a number of trials it was possible to produce fibers at nano and micrometer scale using PHBV and its blends with polylactides. Fiber diameter was found to be affected by many processing parameters but mainly by polymer concentration. The higher the solution viscosity, the higher was the diameter. In the case of electrospun fibers, polymer solution conductivity was found to be a key point for a better fiber structure and morphology. A salt, BTEAC, improved fiber integrity and reduced bead formation, but fiber fusion could not be prevented. On the other hand a small amount of DMF, a solvent with higher dielectric constant than chloroform, was added to chloroform and it improved the results; fibers with a more homogeneous diameter and shape were obtained. In terms of fiber quality blends of PHBV with polylactides yielded the best results, namely the three blends PHBV-PLLA, PHBV-P(L,DL)LA (70:30) and PHBV-PLGA (50:50).

It was also possible, by changing the fiber collector, to obtain aligned nano-/microfibrous scaffolds in diameters not significantly different from that of the random fibers.

One of the main aims of this study was to study the effect of fiber thickness and chemistry on cell spreading, proliferation and differentiation. Therefore, PHBV (10%), PHBV (15%), PHBV-PLLA, PHBV-P(L,DL)LA (70:30), PHBV-PLGA (50:50) blends and wet spun PHBV fibers (15%) were tested with human osteosarcoma cells for their suitability in bone tissue engineering. Wet spun fibers, which had the largest diameters, were not very suitable for cell growth, since the cells did not spread on them.

Electrospun scaffolds were tested as is and after oxygen plasma treatment to investigate the effect of surface oxidation on cell behavior. Plasma treated samples resulted in higher cell numbers and density; however, the difference was not considerable. PHBV-PLLA>PHBV10>PHBV-PLGA(50:50)>PHBV15>PHBV-P(L,DL)LA was the order in terms of cell proliferation rates for the plasma treated fibers. The order was slightly different for the untreated ones; PHBV-PLGA (50:50) and PHBV10 changed their places with the rest staying the same.

Regarding the effect of diameter on cell attachment and based on quantitative results obtained from MTS assay, it was concluded that the lower the fiber diameter, the higher was the number of cells attached on the scaffold. Microscopy studies were also performed to study how the cells interact with other cells and the matrix. These studies showed that generally the cells both spread on the surface and penetrated deep into the interior regions of the fibrous scaffolds. They showed good cell-cell and cell-matrix interactions even in cases where beaded fibers were present, especially with PHBV-PLLA and PHBV-PLGA (50:50) scaffolds.

Another important factor that was considered in this study was the surface porosity of the electrospun scaffolds. It was expected that the higher the surface porosity the better would be the cell distribution and penetration into the interior of the fibrous scaffolds. PHBV-PLLA blend was found to have

the highest porosity and the best proliferation rates and cell spreading. No linear relation, however, was observed between the cell densities and surface porosities. In some cases like that of PHBV10 scaffold, cell density and penetration was found to be satisfactory even though the surface porosity was not that high compared to the others. One complicating factor was the method of determination of the surface porosity. Since it is obtained using image analysis of SEM micrographs, the surface porosity data obtained might not reflect the actual porosity; the nanomat surfaces were probably more porous than the data showed.

As a conclusion, it can be said that biomedical applications, especially tissue engineering, can benefit from these biocompatible and biodegradable electrospun nano-/microfibrous meshes. Fiber properties like thickness, chemistry, uniformity are all very influential along with the porosity of the final scaffold. All the cell loaded constructs produced in this study revealed a significant potential for use in bone tissue engineering with the best performance being with PHBV-PLLA blend. This study needs to be further developed to include polymers with different chemistry or hydrophilicity obtained with more plasma treatment, better methods for characterization of the properties (eg. porosity measurements), and primary cells of human origin.

REFERENCES

1. R. P. Feynman,' There's plenty of room at the bottom', J. Microelectromech. Sys., 1 (1992) 60-66.

2. L. Qian, J. P. Hinestroza, *'Application of Nanotechnology for high performance textiles'*, J Textile Apparel. Technol. Manag., 4, (2004) 1-7.

3. M. E. Gomes, J. S. Godinho, D. Tchalamov, A. M. Cunha, R. L. Reis, *'Alternative tissue engineering scaffolds based on starch: processing methodologies, morphology, degradation and mechanical properties'*, Mater. Sci. Eng. C, 20 (2002) 19-26.

4. M. Li, M. J. Mondrinos, M. R. Gandhi, F. K. Ko, A. S Weiss, P. I. Lelkes, '*Electrospun protein fibers as matrices for tissue engineering*', Biomaterials 26 (2005) 5999-6008.

5. M. Radisic, L. Yang, J. Boublik, R.J. Cohen, R. Langer, L.E. Freed, G. Vunjak-Novakovic, *'Medium perfusion enables engineering of compact and contractile cardiac tissue'*, Am. J. Physiol. Heart. Circ. Physiol., 286, (2004) 507–516.

6. J. Stitzel, J. Liu, S. J. Lee, M. Komura, J. Berry, S. Soker, G. Lim, M. V. Lyke, R. Czerw, J. J. Yoo, A. Atala, *'Controlled fabrication of a biological vascular substitute'*, Biomaterials, 27 (2006) 1088-1094.

7. L. Buttafoco, N. G. Kolkman, P. Engbers-Buijtenhuijs, A. A. Poot, P. J. Dijkstra, I. Vermes and J. Feijen, *'Electrospinning of collagen and elastin for tissue engineering applications'*, Biomaterials, 27 (2006) 724-734.

8. G. Viswanathan, S. Murugesan, V. Pushparaj, O. Nalamasu, P. M. Ajayan, R. J. Linhardt, *'Preparation of biopolymer fibers by electrospinning from room temperature liquids'*, Biomacromol., 7 (2006) 415-418.

9. B. Min, S. W. Lee, J. N. Lim, Y. You, T. S. Lee, P. H. Kang and W. H.Park, '*Chitin and chitosan nanofibers: electrospinning of chitin and deacetylation of chitin nanofibers'*, Polym., 45 (2004) 7137-7142.

10. K. Tuzlakoglu, N. Bolgen, A. J. Salgado, M. E. Gomes, *'Nano- and microfiber combined scaffolds: A new architecture for bone tissue engineering'*, J Mater. Sci.- Mater. Med. 16 (2005) 1099-1104.

11. H. Ylikauppila, L. Nikkola, M. Gomes, R. Reis, N. Ashammakhi, '*Fibrous products in medical and health care*', FiberMed 2006-June 7-9, 2006, Tampere, Finland.

12**.** I. C. Um, D. Fang, B. S. Hsiao, A. Okamoto, B. Chu, '*Electro-spinning and electro-blowing of hyaluronic acid'*, Biomacromol., 5 (2004) 1428-1436.

13. B-M. Min, G. Lee, S. H. Kim, Y. S. Nam, T. S. Lee and W. H. Park, '*Electrospinning of silk fibroin nanofibers and its effect on the adhesion and spreading of normal human keratinocytes and fibroblasts in vitro'*, Biomaterials, 25 (2004) 1289-1297.

14. X. Zong, H. Bien, C. Y. Chung, L. Yin, D. Fang, B. S. Hsiao, B. Chu, E. Entcheva, *'Electrospun fine-textured scaffolds for heart tissue constructs '*, Biomaterials 26 (2005) 5330-5338.

15. K. Kim, M. Yu, X. Zong, J. Chiu, D. Fang, J-S. Seo, B. S. Hsiao, M. Hadjiargyrou, *'Control of degradation rate and hydrophilicity in electrospun non-woven poly(D,L-lactide) nanofiber scaffolds for biomedical applications'*, Biomaterials, 24 (2003) 4977-4985.

16. Y. Zhang, C. T. Lim, S. Ramakrishna, Z. M. Huang, '*Recent development of polymer nanofibers for biomedical and biotechnological applications'*, J Mater. Sci. – Mater. Med., 16 (2005) 933-946.

17. W. K. Son, J. H. Youk, T. S. Lee, W. H. Park, '*The effect of solution properties and polyelectrolyte on electrospinning of ultrafine poly(ethylene oxide) fibers'*, Polym., 45 (2004) 2959-2966.

18. J. S. Choi, S. W. Lee, L. Yong, S. Bae, B. C. Min, J. H. Youk, W. H. Park, *'Effect of oganosoluble salts on the nanofibrous structure of electrospun poly(3-hydroxybutyrate-co-3-hydroxyvalerate)'*, Int. J. Biol. Macromol., 34 (2004) 249-256.

19. G. T. Köse, F. Korkusuz, P. Korkusuz, N. Purali, A. Özkul, V. Hasırcı, *'Bone generation on PHBV matrices: an in vitro study'*, Biomaterials 24 (2003) 4999–5007.

20. G. Q. Chen, Q. Wu, '*The application of polyhydroxyalkanoates as tissue engineering materials'*, Biomaterials 26 (2005) 6565–6578.

21. G. T. Köse, F. Korkusuz, A. Özkul, Y. Soysal, T. Özdemir, C. Yıldız, V. Hasırcı, *'Tissue engineered cartilage on collagen and PHBV matrices'*, Biomaterials 26 (2005) 5187–5197.

22. G. T. Köse, H. Kenar, N. Hasırcı, V. Hasırcı, *'Macroporous poly(3-hydroxybutyrate-co-3-hydroxyvalerate) matrices for bone tissue engineering*', Biomaterials 24 (2003) 1949–1958.

23. M.M. Hohman, M. Shin, G. Rutledge, M. P. Brenner, *'Electrospinning and electrically forced jets. 1. Stability theory'*, Phys. Fluids. 13 (2001) 2201-2220.

24. A. S. Badami, M. R. Kreke, M. S. Thompson, J. S. Riffle, A. S. Goldstein, *'Effect of fiber diameter on spreading, proliferation and differentiation of osteoblastic cells on electrospun poly(lactic acid) substrates'*, Biomaterials 27 (2006) 596-606.

25. F. Yang, R. Murugan, S. Wang, S. Ramakrishna, *'Electrospinning of nano/micro scale poly(lactic acid) aligned fibers and their potential in neural tissue engineering'*, Biomaterials 26 (2005) 2603- 2610.

26. K. Kwon, S. Kidoaki, T. Matsuda, *'Electrospun nano- to microfiber fabrics of biodegradable copolyesters: structural characteristics, mechanical properties and cell adhesion potential'*, Biomaterials, 26 (2005) 3929-3939.

27. X. Zong, K. Kim, D. Fang, S. Ran, B. S. Hsiaoa, B. Chua, *'Structure and process relationship of electrospun bioabsorbable nanofiber membranes'*, Polym., 43 (2002) 4403-4412.

28. C. Xu, F. Yang, S. Wang, S. Ramakrishna, *'In vitro* study of human vascular endothelial cell function on materials with varius surface roughness', J. Biomed. Mater. Res., 71A (2004) 154-161.

29. L. S. Nair, S. Bhattacharyya, J. D. Bender, Y. E. Greish, P. W. Brown, H. R. Allcock, C. T. Laurencin, *'Fabrication and optimization of methylphenoxy substituted polyphosphazane nanofibers for biomedical applications'*, Biomacromol., 5 (2004) 2212-2220.

30. H. Yoshimoto, Y. M. Shin, H. Terai, J. P. Vacanti, *'A biodegradable nanofiber scaffold by electrospinning and its potential for bone tissue engineering'*, Biomaterials 24 (2003) 2077-2082.

31. M. I. van Lieshout, C. M. Vaz, M. C. Rutten, G. W. Peters, F. P. Baaijens, *'Electrospinning versus knitting: two scaffolds for tissue engineering of the aortic valve'*, J. Biomater. Sci. Polym. Ed., 17 (2006) 77-89.

32. M-S- Khil, S. R. Bhattarai, H-Y Kim, S-Z Kim and K-H. Lee, *'Novel fabricated matrix via electrospinning for tissue engineering'*, J. Biomed. Mater. Res. 72B, (2005) 117-124.

33. S. Sahoo, H. Ouyang, J. C. Goh, T. E. Tay, S. L. Toh, *'Characterization of a novel polymeric scaffold for potential application in tendon/ligament tissue engineering'*, Tissue Eng., 12 (2006) 91-99.

34. K. Kim, Y. K. Luu, C. Chang, D. Fang, B. S. Hsiao, B. Chu, M. Hadjiargyrou, *'Incorporation and controlled release of a hydrophilic antibiotic using poly(lactide-co-glycolide)-based electrospun nanofibrous scaffolds'*, J. Controlled Release, 98 (2004) 47-56.

35. W-J. Li, C.T. Laurencin, E. J. Caterson, R. S. Tuan, F. K. Ko, *'Electrospun nanofibrous structure: A novel scaffold for tissue engineering'*, J. Biomed. Mater. Res., 60 (2002) 613-621.

36. C. Y. Xu, R. Inai, M. Kotaki, S. Ramakrishna, *'Aligned biodegradable nanofibrous structure: a potential scaffold for blood vessel engineering'*, Biomaterials 25 (2004) 877-886.

37. X. M. Mo, C. Y. Xu, M. Kotaki, S. Ramakrishna, *'Electrospun P(LLA-CL) nanofiber: a biomimetic extracellular matrix for smooth muscle cell and endothelial cell proliferation'*, Biomaterials, 25 (2004) 1883-1890.

38. C. Xu, R. Inai, M. Kotaki, S. Ramakrishna, *'Electrospun nanofiber fabrication as synthetic extracellular matrix and its potential for vascular tissue engineering'*, Tissue Eng., 10 (2004) 1160-1168.

39. L. Nikkola, J.Sepala, A. Harlin, A. Ndreu, N. Ashammakhi, *'Electrospun multifunctional diclofenac sodium releasing nanoscaffold'*, J. Nanosci. Nanotechnol., 6 (2006) 3290-3295.

40. D. Liang, Y. K. Luu, K. Kim, B. S. Hsiao, M. Hadjiargyrou and B. Chu, *'In vitro non-viral gene delivery with nanofibrous scaffolds'*, Nucleic Acids Res., 33 (2005) 170-183.

41. J. Zeng, A. Aigner, F. Czubayko, T. Kissel, J. H. Wendorff and A. Greiner, *'Poly(vinyl alcohol) nanofibers by electrospinning as a protein delivery system and the retardation of the enzyme release by additional polymer coatings'*, Biomacromol., 6 (2005) 1484-1488.

42. R. El Kenawy, J. M. Layman, J. R. Watkins, G. L. Bowlin, J. A. Matthews, D. G. Simpson, G. E. Wnek, *'Electrospinning of poly(ethylene-co-vinyl alcohol) fibers'*, Biomaterials, 24 (2003) 907-913.

43. K. N. Chua, W. S. Lim, P. Zhang, H. Lu, J. Wen, S. Ramakrishna, K. W. Leongm, H. Q. Mao, *'Stable immobilization of rat hepatocyte spheroids on galactosylated nanofiber scaffold'*, Biomaterials, 26 (2005) 2537-2547.

44. S. Y. Chew, J. Wen, E. K. Yim and K. W. Leong, *'Sustained release of proteins from electrospun biodegradable fibers'*, Biomacromol., 6 (2005) 2017-2024.

45. Y. Z. Zhang, J. Venugopal, Z. M. Huang, C. T. Lim, S. Ramakrishna, '*Characterization of the surface biocompatibility of electrospun PCL-collagen nanofibers using fibroblasts'*, Biomacromol., 6 (2005) 2583-2589.

46. J. J. Stankus, J. Guan, K. Fujimoto, W. R. Wagner,' *Microintegrating smooth muscle cells into a biodegradable, elastomeric fiber matrix'*, Biomaterials, 27 (2006) 735-744.

47. C. Li, C. Vepari, H. J. Jin, H. J. Kim, D. L. Kaplan, *'Electrospun silk-BMP-2 scaffolds for bone tissue engineering'*, Biomaterials 27 (2006) 3115-3124.

48. G. Verreck, I. Chun, J. Rosenblatt, J. Peeters, A. V. Dijck, J. Mensch, M. Noppe, M. E. Brewster, *'Incorporation of drugs in an amorphous state into electrospun nanofibers composed of a water-insoluble, nonbiodegradable polymer'*, J. Controlled Release 92 (2003) 349– 360.

49. J. A. Matthews, G. E. Wnek, D. G. Simpson, G. L. Bowlin, *'Electrospinning of collagen nanofibers'*, Biomacromol., 3 (2002) 232-238.

50. K. S. Rho, L. Jeong, G. Lee, B. M. Seo, Y. J. Park, S. D. Hong, S. Roh, J. J. Cho, W. H. Park, B. M. Min, *'Electrospinning of collagen nanofibers: Effects on the behavior of normal human keratinocytes and early-stage wound healing'*, Biomaterials 27 (2006) 1452–1461.

51. K. J. Shields, M. J. Beckman, G. L. Bowlin and J. S. Wayne, '*Mechanical properties and cellular proliferation of electrospun collagen type* II', Tissue Eng., 10 (2004) 1510-1517.

52. X. Geng, O.-H. Kwon, J. Jang, *'Electrospinning of chitosan dissolved in concentrated acetic acid solution*', Biomaterials 26, (2005) 5427-5432.

53. C. H. Kim, M. S. Khil, H. Y. Kim, H. U. Lee and K. Y. Jahng, '*An improved hydrophilicity via electrospinning for enhanced cell attachment and proliferation'*, J. Biomed. Mater. Res. Part B: Appl. Biomater., 78B (2005) 283-290.

54. H. J. Jin, S. V. Fridrikh, G. C. Rutledge and D. L. Kaplan, *'Electrospinning Bombyx mori silk with poly(ethylene oxide)',* Biomacromol., 3 (2002) 1233-1239.

55. S. Zhong, W. E. Teo, X. Zhu, R. Beuerman, S. Ramakrishna, L. Y. Yung, *'Formation of collagen-glucosaminoglycan blended nanofibrous scaffolds and their biological properties'*, Biomacromol., 6 (2005) 2998-3004.

56. W. He, Z. Ma, T. Yong, W. E. Teo, S. Ramakrishna, '*Fabrication of collagen coated biodegradable polymer mesh and its potential for endothelial cell growth'*, Biomaterials, 26 (2005) 7606-7615.

57. J. Venugopal, L. L. Ma, T. Yong, S. Ramakrishna, *'In vitro study of smooth muscle cells on polycaprolactone and collagen nanofibers'*, Cell Biol. Int., 29 (2005) 861-867.

58. M. Li, Y. Guo, Y. Wei, A.G. Macdiarmid and P. I. Lelkes, *'Electrospinning polyaniline-contained gelatin nanofibers for tissue engineering applications'*, Biomaterials, 27 (2006) 2705-2715.

59. Y. Zhang, H. Ouyang, C. T. Lim, S. Ramakrishna, Z-M. Huang, *'Electrospinning of gelatin fibers and gelatin-PCL composite fibrous scaffolds'*, J. Biomed. Mater. Res., 72 (2005) 156-165.

60. R. Murugan, S. Ramakrishna, *'Nano-featured scaffolds for tissue engineering: A review of spinning methodologies'*, Tissue Eng., 12 (2006) 435-447.

61. R. Langer, *'Selected advances in drug delivery and tissue engineeing',* J. Controlled Release, 62 (1999) 7-11.

62. Y. Fukuhira, E. Kitazono, T. Hayashi, H. Kaneko, M. Tanaka, M. Shimomura, Y. Sumi, *'Biodegradable honeycomb-patterned film composed of poly(lactic acid) and dioleoylphosphatidylethanolamine'*, Biomaterials, 27 (2006) 1797-1802.

63. H. Kenar, G. Torun Köse and V. Hasirci, '*Tissue engineering of bone on micropatterned biodegradable polyester films*', Biomaterials 27(2006) 885-895.

64. R. C. Thomson, M. J. Yaszemski, J. M. Powers, A. G. Mikos, 'Hydroxyapatite fiber reinforced poly(*α*-hydroxy ester) foams for bone regeneration', Biomaterials, 19 (1998) 1935-1943.

65. C. Danielssona, S. Ruaulta, M. Simonet, P. Neuenschwander, P. Frey, *'Polyesterurethane foam scaffold for smooth muscle cell tissue engineering'*, Biomaterials 27 (2006) 1410–1415.

66. Y. Ito, H. Hasuda, M. Kamitakahara, C. Ohtsuki, M. Tanihara, I. K. Kang, O. H. Kwon, *'A composite of hydroxyapatite with electrospun biodegradable nanofibers as a tissue engineering material'*, J Biosci Bioeng. 100 (2005) 43-49.

67. P. Wutticharoenmongkol, N. Sanchavanakit, P. Pavasant, P. Supaphol, *'Preparation and characterization of novel bone scaffolds based on electrospun polycaprolactone fibers filled with nanoparticles'*, Macromol. Biosci. 6 (1) (2005) 70-77.

68. S. R. Bhattarai, N. Bhattarai, H. K. Yi, P. H. Hwang, D. I. Cha, H. Y. Kim, *'Novel biodegradable electrospun membrane: scaffold for tissue engineering'*, Biomaterials 25 (2004) 2595-2602.

69. N. Ashammakhi, A. Ndreu, A. Piras, L. Nikkola, T. Sindelar, H. Ylikauppila, A. Harlin, E. Chiellini, V. Hasirci, H. Redl, *'Biodegradable nanomats produced by electrospinning: expanding multifunctionality and potential for tissue engineering'*, J. Nanosci. Nanotechnol., 6 (2006) 2693-2711.

70. S. Ber, G. T. Kose, V. Hasırcı, '*Bone tissue engineering on patterned collagen films: an in vitro study'*, Biomaterials, 26 (2005) 1977-1986.

71. A. I. Teixeira, G. A. Abrams, P. J. Bertics, C. J. Murphy, P. F. Nealey, '*Epithelial contact guidance on well-defined micro- and nanostructured substrates*', J. Cell Sci. 116 (2003) 1881-1892.

72. Z. M. Huang, Y. Z. Zhang, M. Kotaki, S. Ramakrishna, *'A review on polymer nanofibers by electrospinning and their application in nanocomposites'*, Compos. Sci. Technol., 63, 2223 (2003).

73. J. D. Hartgerink, E. Baniash, S. I. Stupp, '*Self assembly and mineralization of peptide-amphiphile nanofibers'*, Sci., 294 (2001) 1684-1688.

74. Z. Ma, M. Kotaki, R. Inai, S. Ramakrishna, *'Potential of nanofiber matrix as tissue-engineering scaffolds'*, Tissue Eng., 11 (2005) 101-109.

75. J. I. Kroschwitz, '*Encyclopedia of polymer science and engineering'*, 2nd Edn., Vol. 6, John Wiley & Sons, New York, (1986) 812-815.

76. T. Ondarcuhu, C. Joachim, '*Drawing a single nanofiber over hundreds of microns'*, Europhys. Lett., 42 (1998) 215-220.

77. L. Feng, S. Li, H. Li, J. Zhai, Y. Song, L. Yiang, '*Superhydrophobic surface of aligned polyacrylonitrile nanofibers'*, Angew Chem. Int. Ed., 41 (2002) 1221-1223.

78. P. X. Ma, R. Zhang, '*Synthetic nano-scale fibrous extracellular matrix'*, J. Biomed. Mater. Res., 46 (1999) 60-72

79. A. Formhals, US Patent, 2,323,025 (1943).

80. A. Formhals, US Patent, 2,349,950 (1944).

81. A. Formhals, US Patent, 1,975,504 (1934).

82. A. Formhals, US Patent, 2,160,962 (1939).

83. A. Formhals, US Patent, 2,187,306 (1940).

84. J. Kameoka, R. Orth, Y. Yang, D. Czaplewski, R. Mathers, G. W. Coates, H. G. Craighead, *'A scanning tip electrospinning source for deposition of oriented nanofibers'*, Nanotechnol., 14 (2003) 1124-1129.

85. Y. Ji, K. Ghosh, X. Z. Shu, B. Li, J. C. Sokolov, G. D. Prestwitch, R. A. F. Clark, M. H. Rafailovich, *'Electrospun three-dimensional hyaluronic acid nanofibrous scaffolds'*, Biomaterials, 27 (2006) 3782-3792.

86. D. Li and Y. Xia, *'Electrospinning of nanofibers: Reinventing the wheel?'*, Adv. Mater., 16 (2004) 1151-1170.

87. D. H. Reneker, I Chun, *'Nanometre diameter fibers of polymer produced by electrospinning'*, Nanotechnol., 7 (1996) 216-223.

88. R. S. Barhate, C. K. Loong, S. Ramakrishna, *'Preparation and characterization of nanofibrous filtering media'*, J. Membr. Sci., 283 (2006) 209-218.

89. J. M. Deitzel, J. Kleinmeyer, D. Harris, N. C. B. Tan, *'The effect of processing variables on the morphology of electrospun nanofibers and textiles'*, Polym., 42 (2001) 261-272.

90. D. S. Katti, K. W. Robinson, F. K. Ko, and C. T. Laurencin, *'Bioresorbable Nanofiber-Based Systems for Wound Healing and Drug Delivery: Optimization of Fabrication Parameters'*, J. Biomed. Mater. Res. 70B, (2004) 286-96.

91. L. Chun, P. Chen, J. Li, Y. Zhang, *'Computer simulation of electrospinning. Part I. Effect of solvent in electrospinning'*, Polym., 47 (2006) 915-921.

92. A. L. Yarin, S. Koombhongse, D. H. Reneker, *'Bending instability in electrospinning of nanofibers',* J. Appl. Phys., 89 (2001) 3018-3026.

93. K. H. Lee, H. Y. Kim, Y. M. La, D. R. Lee, N. H. Sung, *'Influence of a mixing solvent with tetrahydrofuran and N-dimethylformamide on electrospun poly(vinyl chloride) nonwoven mats'*, J. Polym. Sci.: Part B: Polym. Phys., 40 (2002) 2259-2268.

94. S. Megelski, J. S. Stephens, D. B. Chase and J. F. Rabolt, *'Micro- and nanostructured surface morphology on electrospun polymer fibers'*, Macromol., 35 (2002) 8456-8466.

95. T. Subbiah, G.S. Bhat, R. W. Tock, S. Parameswaran, S. S. Ramkumar, '*Electrospinning of nanofibers'*, J. Appl. Polym. Sci., 96 (2005) 557-569.

96. M.M. Demir, I.Yilgor, E. Yilgor, B. Erman, '*Electrospinning of polyurethane fibers'*, Polym., 43 (2002) 3303-3309.

97. C. L. Casper, J. S. Stephens, N. G. Tassi, B. D. Chase, J. F. Rabolt, *'Controlling surface morphology of electrospun polystyrene fibers: Effect of humidity and molecular weight in the electrospinning process'*, Macromol., 37 (2004) 573-578.

98. C. J. Buchko, L. C. Chen, Y. Shen, D. C. Martin, *'Processing and microstructural characterization of porous biocompatible protein polymer thin films'*, Polym., 40 (1999) 7397-7407.

99. U. Boudriot, R. Dersch, A.Greiner, J. H.Wendorff, '*Proceedings Nanotechnology in Science, Economy, and Society*', January 13-15 (2005) Marburg, Germany.

100. M. G. McKee, M. T. Hunley, J. M. Layman, T. E. Long, '*Solution rheological behavior and electrospinning of cationic polyelectrolytes'*, Macromol., 39 (2006) 575-583.

101. N. Bolgen , Y. Z. Menceloglu, K. Acatay, I. Vargel, E. Piskin, *'In vitro and in vivo degradation of non-woven materials made of poly(ε-caprolactone) nanofibers prepared by electrospinning under different conditions'*, J. Biomater. Sci. Polym. Ed., 16 (2005) 1537-1555.

102. A. Piras, L. Nikkola, F. Chiellini, E. Chiellini, N. Ashammakhi, *'Development of diclofenac sodium releasing bio-erodible polymeric nanomats'*, J. Nanosci. Nanotech., 6 (2006) 3310-3320.

103. Y. Wang, D. I. Blasioli, H. Kim, H. S. Kim, D. L. Kaplan, '*Cartilage tissue engineering with silk scaffolds and human articular chondrocytes'*, Biomaterials, 27 (2006) 4434-4442.

104. H. J. Shin, C. H. Lee, I. H. Cho, Y. J. Kim, Y. J. Lee, I. A. Kim, K. D. Park, N. Yui, '*Electrospun PLGA nanofiber scaffolds for articular cartilage reconstruction: mechanical stability, degradation and cellular responses under mechanical stimulation in vitro'*, J Biomater. Sci. Polym. Edn., 17 (2006) 103-119.

105. M. Shin, H. Yoshimoto, J. P. Vacanti, *'In vivo bone tissue engineering using mesenchymal stem cells on a novel electrospun nanofibrous scaffold'*, Tissue Eng., 10 (2004) 33-41.

106. H. K. Noh, S. W. Lee, J. M. Kim, J. E. Oh, K. H. Kim, C. P. Chung, S. C. Choi, W. H. Park, B. M. Min, *'Electrospinning of chitin nanofibers: Degradation behavior and cellular response to normal human keratinocytes and fibroblasts'*, Biomaterials, 27 (2006) 3934-3944.

107. A. Frenot, I. S. Chronakis, *'Polymer nanofibers assembled by electrospinning'*, Current Opinion in Colloid and Interface Sciences, 8 (2003) 64-75.

108. S. A. Riboldi, M. Sampaolesi, P. Neunenschwander, G. Cossu, S. Mantero, *'Electrospun degradable polyesterurethane membranes: potential scaffolds for skeletal muscle tissue engineering'*, Biomaterials 26 (2005) 4606-4615.

109. A. Atala, R. P. Lanza, *'Methods of tissue engineering'*, Chapter 25, Pg. 317-330, Academic Press 2002, California, USA.

110. P. Bianco, P.G Robey, *'Stem cells in tissue engineering'*, Nature, 414 (2001) 117-121.

111. Z. Ma, W. He, T. Yong, S. Ramakrishna, *'Grafting of gelatin on electrospun poly(caprolactone) nanofibers to improve endothelial cell spreading and proliferation and to control cell orientation'*, Tissue Eng., 11 (2005) 1149-1158.

112. C. H. Lee, H. J. Shin, I. H. Cho, Y. M. Kang, I. A. Kim, K. D. Park, J. W. Shin, *'Nanofiber alignment and direction of mechanical strain affect the ECM production of human ACL fibroblast'*, Biomaterials, 26 (2005) 1261-1270.

113. K. Fujihara, M. Kotaki, S. Ramakrishna, *'Guided bone regeneration membrane made of polycaprolactone/calcium carbonate composite nanofibers'*, Biomaterials, 26 (2005) 4139-4147.

114. Q. F. Wei, W. D. Gao, D. Y. Hou, X. Q. Wang, *'Surface modification of polymer nanofibers by plasma treatment'*, Appl. Surf. Sci., 245 (2005) 16-20.

115. Y. Wang, L. Lu, Y. Zheng, X. Chen, *'Improvement in hydrophilicity of PHBV films by plasma treatment'*, J. Biomed. Mater. Res. - Part A, 76 (2006) 589-595.

116. L. Moroni, R. Licht, J. de Boer, J. R. de Wijn, C. A. van Blitterswijk, *'Fiber diameter and texture of electrospun PEOT/PBT scaffolds influence*

human mesenchymal stem cell proliferation and morphology, and the release of incorporated compounds', Biomaterials, 27 (2006) 4911-4922.

117. S. J. Kim, C. K. Lee, S. I. Kim, *'Effect of ionic salts on the processing of Poly(2- acryloamido-2-methyl-1-propane sulfonic acid) nanofibers'*, J. Apl. Polym. Sci., 96 (2005) 1388-1393.

118. S. C. Baker, N. Atkin, P. A. Gunning, N. Granville, K. Wilson, D. Wilson, J. Southgate, *'Characterization of electrospun polystyrene scaffolds for three-dimensional in vitro biological studies'*, Biomaterials, 27 (2006) 3136-3146.

119. C. K. Lee, S. I. Kim, S. J. Kim, *'The influence of added ionic salt on nanofiber uniformity for electrospinning of electrolyte polymer'*, Synth. Met., 154 (2005) 209-212.

APPENDIX

APPENDIX A

Figure A.1. Calibration curve of MTS assay for human osteosarcoma cells (SaOs-2).